THE ASTROPHYSICAL JOURNAL, 427:202–220, 1994 May 20

THE NUCLEAR 10 MICRON EMISSION OF SPIRAL GALAXIES

GIULIANO GIURICIN,[1,2,3] LAURA TAMBURINI,[1,2,4] FABIO MARDIROSSIAN,[1,2,5]
MARINO MEZZETTI,[1,2,6] AND PIERLUIGI MONACO[1,2,7]
Received 1993 June 16; accepted 1993 October 21

ABSTRACT

We examine the 10 μm emission of the central regions of 281 spiral galaxies, after having compiled all ground-based, small-aperture ($\sim 5''$) broad-band photometric observations at $\lambda \sim 10$ μm (N magnitudes) published in the literature. We evaluate the compactness of the ~ 10 μm emission of galaxy nuclei by comparing these small-beam measures with the large-beam *IRAS* 12 μm fluxes. In the analysis of different subsets of objects, we apply survival analysis techniques in order to exploit the information contained in "censored" data (i.e., upper limits on the fluxes).

Seyfert galaxies are found to contain the most powerful nuclear sources of mid-infrared emission, which in approximately one-third of the cases provide the bulk of the emission of the entire galaxy; thus, mid-infrared emission in the outer disk regions is not uncommon in Seyfert galaxies. The 10 μm emission of Seyfert galaxies appears to be unrelated to their X-ray emission.

H II region–like nuclei are stronger mid-infrared sources than normal nuclei and LINER nuclei (whose level of emission is not distinguishable from that of normal nuclei). Interacting objects have, on average, greater 10 μm luminosities than noninteracting ones and exhibit more compact emission. Early-type spirals have stronger and more compact 10 μm emission than late-type ones. Barred spirals are brighter at ~ 10 μm than unbarred systems, essentially because they more frequently contain H II region–like nuclei.

The results of our detailed comparison between the behavior of various categories of objects stress that the 10 μm emission of spiral nuclei is closely linked to the (predominantly nonthermal synchrotron) radio emission.

Subject headings: galaxies: nuclei — galaxies: Seyfert — infrared: galaxies — galaxies: photometry — galaxies: spiral

1. INTRODUCTION

Ground-based, small-aperture mid-infrared (MIR) photometric observations have shown that the nuclei of spiral galaxies are often bright at these wavelengths. Large observational efforts were performed particularly by Rieke & Lebofsky (1978), Lonsdale, Persson, & Mathews (1984), Lawrence et al. (1985), Willner et al. (1985), Cutri & McAlary (1985), Devereux, Becklin, & Scoville (1987), Devereux (1987), Ward et al. (1987), Carico et al. (1988), Wright et al. (1988), Hill, Becklin, & Wynn-Williams (1988), and Wynn-Williams & Becklin (1993). Strong MIR emission from galactic nuclei, which is clearly indicative of nonstellar radiation, is frequently observed in Seyfert and starburst nuclei (see, e.g., the review by Rieke & Lebofsky 1979), in several LINER nuclei (Lawrence et al. 1985; Willner et al. 1985), in interacting and merging galaxies (Lonsdale et al. 1984; Cutri & McAlary 1985; Joseph & Wright 1985; Wright et al. 1988), with no obvious dependence on the spiral morphological type (Devereux et al. 1987), although it has been claimed to be related to the presence of a bar, in early-type spirals (Devereux 1987). For a few galaxies mapped at fairly high resolution at MIR and radio wavelengths, the emission at $\lambda \sim 10$ μm shows a good overall spatial correlation with the (thermal and nonthermal) radio emission (see, e.g., the review by Telesco 1988).

The MIR emission is generally attributed to thermal radiation from warm dust which has been heated by early-type stars formed in a recent burst of star formation, by shocks in supernova remnants, and/or by a central dust-enshrouded active galactic nucleus (AGN) (see, e.g., Ho et al. 1989 and the review by Telesco 1988); in the case of AGNs, the presence of a important nonthermal power-law MIR emission component is conceivable, especially in the high-luminosity objects, although in recent years its role has tended to be deemphasized with respect to the thermal radiation (see, e.g., the review by Bregman 1990).

Spectroscopic observations in the MIR spectral band have revealed remarkable differences in the main spectral properties of different categories of galactic nuclei. The nuclei dominated by H II regions exhibit prominent narrow emission features in the 3–13 μm spectral interval, the so-called unidentified infrared bands (UIR); these bands are generally absent in AGNs, which usually have either featureless MIR spectra or spectra characterized by a strong silicate absorption band at $\lambda \sim 9.7$ μm. (Roche et al. 1991).

In view of the remarkable separation of the MIR spectra of different categories of galactic nuclei, it is worthwhile to explore in detail how the strength of the nuclear mid-infrared luminosity depends on the type of galactic nucleus and on other characteristics of the host galaxy. This has not been adequately examined in earlier MIR studies, although valuable efforts in this direction have been already performed especially by Devereux et al. (1987), Devereux (1987), and Hill et al. (1988). Our investigation can help us to cast more light on the nature of MIR emission in different classes of objects.

[1] Scuola Internazionale Superiore di Studi Avanzati (SISSA), via Beirut 4, 34013 Trieste, Italy.
[2] Dipartimento di Astronomia, Università degli studi di Trieste, via Tiepolo 11, 34131 Trieste, Italy.
[3] E-mail: giuricin@tsmi19.sissa.it.
[4] E-mail: tamburini@tsmi19.sissa.it.
[5] E-mail: mardirossian@tsmi19.sissa.it.
[6] E-mail: mezzetti@tsmi19.sissa.it.
[7] E-mail: monaco@tsmi19.sissa.it.

In this paper, with the aim of providing a comprehensive picture of the MIR activity in galactic nuclei, we examine the MIR emission of an extensive sample of spiral galaxy nuclei. In § 2 we present the adopted galaxy sample and the small-aperture MIR (at ~10 μm) photometric data that we have compiled from the literature. In § 3, adopting a statistical approach, we submit well-defined subsets of objects to a rigorous comparative analysis; we use survival analysis techniques in order to exploit the information in censored data (i.e., MIR fluxes). In § 4 we discuss the main results of our various two-sample comparisons and we address the relation between 10 μm and X-ray emissions in Seyfert galaxies. Section 5 contains our conclusions.

2. THE DATA SAMPLE

We have constructed our galaxy sample by choosing the spiral galaxies listed in the Nearby Galaxies Catalog (NBG) by Tully (1988) with tabulated distance less than 40 Mpc. This volume-limited catalog is intended to include essentially all known optically bright galaxies with systemic recession velocities of less than 3000 km s^{-1}. This corresponds to a distance of 40 Mpc for the Hubble constant $H_0 = 75$ km s^{-1} Mpc^{-1}, which value is adopted throughout this paper. In the NBG catalog the distances of all noncluster galaxies have been essentially estimated on the basis of velocities, an assumed H_0 as above, and the Virgocentric retardation model described by Tully & Shaya (1984), in which the authors assume that the Milky Way is retarded by 300 km s^{-1} from the universal Hubble flow by the mass of the Virgo Cluster. The galaxy members of clusters have been given a distance consistent with the mean velocity of the cluster.

From the literature we have gathered together all published ground-based, small-aperture, broad-band photometric measures at ~10 μm (N magnitudes) for our galaxy sample. For the old literature we have consulted the reference sources cited in the catalog by de Vaucouleurs & Longo (1988). In view of the fairly large uncertainties associated with the N fluxes (which are generally not smaller than 20%) no corrections have been applied for the redshift and the interstellar extinction. The central 10 μm luminosity (in solar units) is evaluated using the expression

$$L_N = 8000 F_N D^2 , \quad (1)$$

where F_N is the 10 μm flux measured in units of millijanskys and D is the distance in units of megaparsecs (Scoville et al. 1983).

Table 1 lists the galaxies of our sample for which small-aperture N data (or upper limits) are available in the literature, together with the morphological type T, bar type (SA, SAB, SB), and ring type S(r), S(rs), S(s) as coded in the RC3 catalog (de Vaucouleurs et al. 1991), the adopted distance D (in Mpc) as tabulated in NBG, the decimal logarithm of the central luminosity L_N (in solar units) for detected objects or an upper (2 σ) limit for undetected galaxies, the projected linear size A of the central region (in kpc) corresponding to the beam size (mostly around 5″–6″) used in the observations, the reference source for photometry, the classification of the nuclear emission-line spectrum as follows: H = H II region–like, L = LINER, S1 = Seyfert 1, S2 = Seyfert 2, S = Seyfert; L/S (which indicates an uncertain classification of the AGN spectrum); L/H (which indicates a composite AGN/H II region–like nucleus in which the latter component is largely dominant over a weak AGN); T (which indicates objects of transition between H and L). The interacting galaxies are denoted by INT. For the galaxies detected by the *Infrared Astronomical Satellite* (*IRAS*) in the 12 μm band, in the last column we list the ratio (or its upper limit) of the ground-based small-beam 10 μm flux to the larger beam *IRAS* 12 μm flux, color-corrected to 10 μm. The resulting compactness parameter C, which indicates the degree to which the central region contributes to the MIR emission of the whole galaxy, is calculated (following Devereux 1987) as

$$C = (F_{10\mu m}/F_{12\mu m}) f_{cc} , \quad (2)$$

where the color correction factor f_{cc} is related to the ratio between the *IRAS* 25 and 12 μm fluxes via the following relation proposed by Devereux (1987):

$$f_{cc} = (0.12 F_{25\mu m}/F_{12\mu m}) + 1.04 . \quad (3)$$

In a few cases in which we unreasonably obtain $C > 1$, we simply adopt $C = 1$. Typical uncertainties in C (due to errors on fluxes) are on the order of 0.1.

We have included in our sample also a few galaxies with $T = -1$ (according to the RC3 catalog), which sometimes in the past have been classed as early-type spirals. Priority is generally given to the most recent photometry and to the measurements made with a beam size corresponding to a physical size of about 0.5–1 kpc (which is typical for most of the data).

For classification of the optical nuclear spectra we have generally relied on the spectroscopic surveys of Stauffer (1982), Keel (1983, 1984), Keel et al. (1985), Véron-Cetty & Véron (1986), Huchra & Burg (1992), the list of starburst nuclei compiled by Balzano (1983), the list of bona fide LINERs culled by Willner et al. (1985), the catalogs of Markarian objects by Mazzarella & Balzano (1986), the listing of Durret (1989), and the catalog of AGNs by Véron-Cetty & Véron (1991). According to the widely used classification precepts of Baldwin, Phillips, & Terlevich (1981), the emission line strength ratios Hα/[N II] λ6584 and [O III] λ5007/Hβ are used in order to distinguish Seyfert, LINER, and H II region-like nuclei; for instance, generally the H II region–like nuclei are characterized by line strength ratios Hα/[N II] λ6584 > 0.7 and [S II] λλ6717, 6731/Hα < 0.4, whereas LINERS have [N II] λ6584 appreciably stronger than Hα and [O III] λ5007/Hβ < 3. The unclassified nuclei are either objects with nuclear spectra without emission lines or (mostly) objects with unobserved nuclear spectra. A discrete fraction of the latter objects are likely to be LINERs in the early-type spiral morphological range and H II nuclei in the late-type interval, owing to the known preference of the two classes of nuclei to reside in early- and late-type spirals, respectively (see, e.g., Keel 1983).

We have denoted as interacting the galaxies listed in the Atlas and Catalogue of Interacting Galaxies by Vorontsov-Vel'yaminov (1959, 1977), the interacting galaxies culled by Davis & Seaquist (1983) essentially from the UGC catalog (Nilson 1973), the objects listed in the complete sample of interacting galaxies surveyed by Keel et al. (1985) and in the sample of violently interacting galaxies studied by Bushouse (1986, 1987), the paired galaxies listed in the Catalogue of Isolated Pairs of Galaxies in the Northern Hemisphere (Karachentsev 1972, 1987), the binary galaxies selected by White et al. (1983) and by Schweizer (1987), the twin galaxies identified by Yamagata, Noguchi, & Iye (1989). Our subsample of interacting galaxies is likely to be skewed toward pairs of galaxies which are close to one another, independently of their morphological appearance (several galaxy pairs show no evidence of tidal

TABLE 1

THE DATA SAMPLE

Name	Type	D (Mpc)	log $L_N(L_\odot)$	A (kpc)	Reference	Class	C
N7817.....	4 SA	31.5	<8.71	0.84	1	...	<0.16
N157.....	4 SX T	20.9	<8.22	0.56	1	T	<0.04
N224.....	3 SA S	0.7	4.99	0.02	2	...	0.0002
N247.....	7 SX S	2.1	<6.54	0.06	2	...	...
N253.....	5 SX S	3.0	8.88	0.19	3	L/H	0.43
N337.....	7 SB S	20.7	<8.01	0.55	1	H	<0.09
N470.....	3 SA T	30.5	9.12	0.81	1	H INT	0.62
N520.....		27.8	<8.17	0.74	4	H INT	<0.04
N598.....	6 SA S	0.7	<5.59	0.02	2	...	<0.01
N628.....	5 SA S	9.7	<7.64	0.27	2	...	<0.03
N660.....	1 SB S	11.8	9.00	0.46	5	T INT	0.43
N701.....	5 SB T	22.7	<8.30	0.61	1	...	<0.10
N908.....	5 SA S	17.8	8.06	0.47	1	H	0.03
N1022.....	1 SB S	18.5	9.01	0.49	1	...	0.82
Maffei 2.....	4 SX T	3.4	7.99	0.07	6	H	0.39
N1068.....	3 SA T	14.4	10.62	0.40	2	S2	0.91
N1084.....	5 SA S	17.1	8.30	0.46	1	H	0.05
N1087.....	5 SX T	19.0	<8.27	0.51	1	H	<0.07
N1097.....	3 SB S	14.5	8.04	0.35	7	L INT	0.03
I277.....	4 SB T	34.2	9.06	0.91	1	H INT	1.
N1187.....	5 SB R	16.3	8.58	0.43	1	H	0.22
N1232.....	5 SX T	20.0	<8.35	0.55	2	...	<0.10
I342.....	6 SX T	3.9	8.29	0.34	8	H	0.09
N1241.....	3 SB T	26.6	8.69	0.71	1	S2 INT	0.19
N1309.....	4 SA S	26.0	<8.31	0.69	1	...	<0.11
I1953.....	4 SB T	22.1	8.37	0.59	1	...	0.34
N1365.....	3 SB S	16.9	8.92	0.45	1	S1 INT	0.11
N1386.....	−1 SB S	16.9	8.68	0.45	1	S2	0.58
N1385.....	6 SB S	17.5	<7.89	0.47	1	H	<0.03
N1415.....	0 SX S	17.7	<8.19	0.47	1	...	<0.13
N1421.....	4 SX T	25.5	<8.16	0.68	1	H	<0.04
N1784.....	5 SB R	28.7	<8.52	0.77	1	L	<0.16
N1808.....	1 SX S	10.8	9.35	0.66	9	S2	0.87
N1832.....	4 SB R	23.5	<8.36	0.63	1	H	<0.09
N1964.....	3 SX S	20.0	<8.24	0.53	1	...	<0.08
I438.....	5 SA T	39.0	<8.47	1.04	1	...	<0.13
N2139.....	6 SX T	22.4	<8.30	0.60	1	H	<0.21
I2166.....	4 SX S	38.9	<8.43	1.04	1	...	<0.14
N2273.....	1 SB R	28.4	9.08	0.76	1	S2	0.58
N2654.....	2 SB	23.3	<8.11	0.62	10	...	...
N2683.....	3 SA T	5.7	<7.32	0.16	2	L	<0.09
N2681.....	0 SX T	13.3	8.11	0.38	11	L/S	0.30
N2708.....	3 SX S	27.8	<8.41	0.74	1	...	<0.29
N2712.....	3 SB R	28.6	<8.29	0.76	1	...	<0.16
N2750.....	5 SX	38.4	8.95	1.02	1	H INT	0.60
N2742.....	5 SA S	22.2	<8.07	0.59	10	INT	<0.13
N2775.....	2 SA R	17.0	<7.84	0.45	10	L	...
N2776.....	5 SX T	38.7	<8.46	1.03	1	H	0.21
N2782.....	1 SX T	37.3	9.10	0.99	1	H	0.21
N2798.....	1 SB S	27.1	9.05	0.66	12	H INT	0.38
N2844.....	1 SA R	24.1	<8.14	0.64	10	...	...
N2841.....	3 SA R	12.0	<7.21	0.35	13	L	<0.02
N2893.....	0 SB T	26.8	8.52	0.71	1	H	0.45
N2903.....	4 SX T	6.3	7.84	0.18	11	H	0.05
N2935.....	3 SX S	30.6	<8.32	0.82	1	...	<0.06
N2967.....	5 SA S	30.9	<8.39	0.82	1	...	<0.06
N2964.....	4 SX R	21.9	8.69	0.58	1	H INT	0.22
N2992.....	1	30.5	9.28	0.81	4	S INT	0.57
N2993.....	1	30.5	8.51	0.81	4	L INT	...
N3003.....	4	24.4	<8.18	0.65	1	...	<0.27
N3023.....	5 SX S	27.6	<8.34	0.74	1	INT	<0.37
N3021.....	4 SA T	25.1	<8.15	0.67	1	...	<0.10
N3041.....	5 SX T	22.8	<8.10	0.61	10	...	...
N3044.....	5 SB S	20.6	8.15	0.55	1	...	0.09
N3031.....	2 SA S	1.4	6.13	0.03	2	L INT	0.02
N3034.....	90	5.2	9.77	0.76	14	H INT	0.57
N3055.....	5 SX S	26.9	8.33	0.72	1	...	0.17
N3067.....	2 SX S	24.2	8.42	0.65	1	...	0.11
N3079.....	5 SB S	20.4	8.48	0.56	1	L	0.04
N3077.....	90	2.1	8.07	0.06	15	H INT	1.

TABLE 1—*Continued*

Name	Type	D (Mpc)	log $L_N(L_\odot)$	A (kpc)	Reference	Class	C
N3162.....	4 SX T	22.2	<8.07	0.59	10	...	...
N3166.....	0 SX T	22.0	8.31	0.59	1	L INT	0.19
N3169.....	1 SA S	19.7	8.50	0.53	1	L INT	0.09
N3177.....	3 SA T	21.1	8.53	0.56	1	...	0.18
N3190.....	1 SA S	22.4	<8.11	0.60	1	L INT	<0.11
N3227.....	1 SX S	20.6	8.95	0.55	10	S1 INT	0.36
N3256.....		37.4	10.22	2.72	16	H INT	0.85
N3254.....	4 SA S	23.6	<8.13	0.63	10	...	...
U5720.....	10	24.9	8.69	0.72	15	H	...
N3277.....	2 SA R	25.0	<8.18	0.67	10	...	...
N3287.....	7 SB S	20.6	<8.01	0.55	10	...	...
N3294.....	5 SA S	26.7	<8.17	0.71	1	...	<0.03
N3310.....	4 SX R	18.7	8.45	0.50	1	H INT	0.09
N3338.....	5 SA S	22.8	<8.10	0.61	10	L	...
N3351.....	3 SB R	8.1	7.32	0.22	10	H	0.05
N3368.....	2 SX T	8.1	7.25	0.23	11	L	0.04
N3370.....	5 SA S	23.4	8.17	0.62	1	...	0.13
N3395.....	6 SX T	27.4	8.21	0.77	17	H INT	...
N3396.....	10 SB	28.0	8.55	0.79	17	H INT	...
N3430.....	5 SX T	26.7	<8.23	0.71	1	H INT	...
N3437.....	5 SX T	23.4	8.36	0.62	1	...	0.09
N3448.....	90	24.5	<8.43	0.65	4	INT	<0.32
N3486.....	5 SX R	7.4	<7.72	0.20	2	L	<0.21
N3504.....	2 SX S	26.5	9.35	0.71	1	H	0.53
N3512.....	5 SX T	25.0	<8.18	0.67	10	...	...
N3521.....	4 SX T	7.2	<6.82	0.21	11	L	<0.01
I2627.....	4 SA S	29.5	<8.44	0.79	1	...	<0.12
N3568.....	5 SB S	32.7	<8.38	0.87	1	...	<0.07
N3583.....	3 SB S	34.0	8.71	0.91	1	...	0.10
N3596.....	5 SX T	23.0	<8.10	0.61	10	...	...
N3611.....	1 SA S	27.3	8.65	0.73	1	INT	0.27
N3623.....	1 SX T	7.3	<7.28	0.20	2	L INT	...
N3627.....	3 SX S	6.6	7.58	0.18	2	L INT	0.03
N3631.....	5 SA S	21.6	<8.08	0.58	1	H INT	<0.03
N3655.....	5 SA S	26.5	<8.25	0.71	1	...	<0.06
N3672.....	5 SA S	28.4	8.33	0.76	1	H	0.04
N3675.....	3 SA S	12.8	<7.59	0.34	10	...	<0.02
N3683.....	5 SB S	28.4	8.57	0.76	1	...	0.06
N3686.....	4 SB S	23.5	<8.18	0.63	1	...	<0.11
N3717.....	3 SA	24.6	<8.37	0.66	1	H	<0.05
N3718.....	1 SB S	17.0	<7.84	0.45	10	L INT	<0.23
N3729.....	1 SB R	17.0	7.93	0.45	10	INT	...
N3732.....	0 SX S	26.9	8.27	0.72	1	...	0.13
N3756.....	4 SX T	23.5	<8.12	0.63	10	...	...
N3783.....	1 SB R	38.5	9.77	1.03	1	S1	0.90
N3810.....	5 SA T	16.9	<7.86	0.45	1	H	<0.03
N3813.....	3 SA T	26.4	8.37	0.70	10	...	...
N3885.....	0 SA S	27.8	8.64	0.74	1	...	0.24
N3887.....	4 SB R	19.3	<8.01	0.51	1	...	<0.06
N3888.....	5 SX T	37.5	8.58	1.00	1	INT	0.11
N3893.....	5 SX T	17.0	<7.84	0.45	1	INT	<0.02
N3949.....	4 SA S	17.0	<8.01	0.45	1	...	<0.07
N3982.....	3 SX R	17.0	<8.01	0.45	1	S2	<0.1
N3992.....	4 SB T	17.0	<8.06	0.47	2	L	...
N4027.....	8 SB S	25.6	8.28	0.68	1	H INT	0.05
N4030.....	4 SA S	25.9	8.33	0.69	1	...	0.03
N4037.....	3 SB T	17.2	<7.88	0.50	10	...	...
N4038.....	9 SB S	25.5	8.27	0.68	4	H INT	...
N4041.....	4 SA T	22.7	<8.22	0.61	1	...	<0.04
N4051.....	4 SX T	17.0	8.88	0.45	1	S1	0.29
N4064.....	1 SB S	16.9	<7.86	0.49	10	...	<0.20
N4088.....	4 SX T	17.0	<7.90	0.45	1	H INT	<0.02
N4096.....	5 SX T	8.8	<7.13	0.26	18	L	<0.03
N4100.....	4 SA T	17.0	7.97	0.45	1	H	0.07
N4102.....	3 SX S	17.0	9.24	0.45	1	L	0.64
N4124.....	−1 SA R	16.8	<7.73	0.45	10	...	...
N4151.....	2 SX T	20.3	9.66	0.58	21	S1.5 INT	1.
N4152.....	5 SX T	34.5	8.65	0.92	1	H	0.13
N4157.....	3 SX S	17.0	<8.06	0.45	1	...	<0.03
N4162.....	4 SA T	38.5	8.40	1.03	1	...	0.13
N4178.....	8 SB T	16.8	<7.86	0.49	10	...	<0.13
N4192.....	2 SX S	16.8	7.79	0.45	10	L	0.03

TABLE 1—*Continued*

Name	Type	D (Mpc)	log $L_N(L_\odot)$	A (kpc)	Reference	Class	C
N4189.....	6 SX T	16.8	8.03	0.45	10	...	0.15
N4194.....	9 SB	39.1	9.66	1.04	1	H INT	0.76
1212-35	3 SB S	36.5	9.08	0.97	1	...	0.61
N4212.....	4 SA	16.8	8.03	0.45	1	H	0.07
N4214.....	10 SX S	3.5	<6.92	0.10	2	H	<0.21
N4216.....	3 SX S	16.8	<7.86	0.49	10	L	<0.05
N4237.....	4 SX T	16.8	<7.86	0.49	10	...	<0.10
N4254.....	5 SA S	16.8	<7.89	0.49	1	H	<0.01
N4258.....	4 SX S	6.8	7.64	0.19	11	L INT	0.06
N4273.....	5 SB S	35.1	8.84	0.94	1	H INT	0.12
N4293.....	0 SB S	17.0	8.05	0.45	10	L	0.17
N4294.....	6 SB S	16.8	<7.86	0.49	10	INT	<0.27
N4298.....	5 SA T	16.8	<7.86	0.49	10	INT	<0.04
N4303.....	4 SX T	15.2	8.17	0.41	1	L	0.03
N4307.....	3	16.8	<7.86	0.49	10	...	<0.42
N4304.....	4 SB S	36.0	8.90	0.96	1	H	0.20
N4314.....	1 SB T	9.7	<7.38	0.28	10	L	...
N4321.....	4 SX S	16.8	7.96	0.45	1	...	0.02
I3253.....	5 SA S	37.0	<8.86	0.99	1	H	<0.22
N4369.....	1 SA T	21.6	8.12	0.58	1	H	0.16
N4380.....	3 SA T	16.8	<7.86	0.49	10	...	<0.20
N4385.....	−1 SB T	33.5	9.05	0.89	1	H	0.61
N4388.....	3 SA S	16.8	8.96	0.49	10	S2	0.54
N4394.....	3 SB R	16.8	<7.86	0.49	10	L INT	0.13
N4412.....	3 SB R	35.6	<8.48	0.95	1	...	...
N4419.....	1 SB S	16.8	8.52	0.45	1	L	0.27
N4424.....	1 SB S	16.8	7.91	0.45	10	...	0.26
N4438.....	0 SA S	16.8	8.09	0.49	10	L INT	0.37
N4450.....	2 SA S	16.8	<7.86	0.49	10	L	<0.25
N4457.....	0 SX S	17.4	8.02	0.51	10	L	0.18
N4469.....	0 SB S	16.8	8.06	0.49	10	...	0.64
N4490.....	7 SB S	7.8	<7.24	0.22	2	H INT	<0.03
N4496.....	6	13.1	<7.64	0.38	10	INT	<0.17
N4501.....	3 SA T	16.8	<7.89	0.45	1	L	<0.02
N4519.....	7 SB T	16.8	<7.86	0.49	10	...	<0.15
N4527.....	4 SX S	29.3	8.94	0.78	1	T	0.06
N4532.....	10 SB	15.5	<7.89	0.41	1	...	<0.19
N4535.....	5 SX S	16.8	8.23	0.45	1	H	0.08
N4536.....	4 SX T	13.3	8.51	0.39	10	...	0.19
N4548.....	3 SB T	16.8	<7.86	0.49	10	L	<0.09
N4559.....	6 SX T	9.7	<7.58	0.27	2	H	<0.07
N4561.....	8 SB T	12.3	<7.59	0.36	10	INT	...
N4565.....	3 SA S	9.7	<7.63	0.27	2	L	<0.05
N4567.....	4 SA T	16.8	<7.86	0.49	10	H INT	...
N4568.....	4 SA T	16.8	8.15	0.49	10	H INT	0.04
N4569.....	2 SX T	16.8	8.48	0.49	1	L INT	0.12
N4571.....	6 SA R	16.8	<8.15	0.49	10	...	<0.09
N4579.....	3 SX T	16.8	8.15	0.49	10	L	0.06
N4580.....	1 SX T	25.6	<8.22	0.74	10	...	<0.12
N4586.....	1 SA S	17.5	7.98	0.51	10	...	...
N4593.....	3 SB T	39.5	9.40	1.05	1	S1	0.73
N4594.....	1 SA S	20.0	8.02	0.58	18	L	0.04
N4595.....	3 SX T	16.8	<8.15	0.49	10	...	<0.40
N4602.....	4 SX T	37.9	<8.30	1.01	1	H	<0.03
N4639.....	4 SX T	16.8	<8.15	0.49	10	S1	...
N4643.....	0 SB T	25.7	<8.07	0.74	11	L	...
N4647.....	5 SX T	16.8	<7.86	0.49	10	H INT	<0.04
N4651.....	5 SA T	16.8	7.87	0.49	10	L INT	0.09
N4654.....	6 SX T	16.8	<7.89	0.45	1	H	<0.04
N4658.....	4 SB S	35.7	<8.42	0.95	1	H	<0.11
N4689.....	4 SA T	16.8	<7.86	0.49	10	H	<0.08
N4691.....	0 SB S	22.5	8.66	0.60	1	H	0.20
N4698.....	2 SA S	16.8	<7.86	0.49	10	L	<0.14
N4699.....	3 SX T	25.7	<8.07	0.74	1	L	<0.03
N4710.....	−1 SA R	16.8	7.99	0.45	1	...	0.12
N4713.....	7 SX T	17.9	<7.91	0.52	10	...	<0.15
N4725.....	2 SX R	12.4	7.95	0.33	10	L	0.25
N4736.....	2 SA R	4.3	7.24	0.12	11	L	0.03
N4747.....	6 SB	12.3	<7.56	0.33	10	...	...
N4775.....	7 SA S	26.6	<8.23	0.71	1	...	<0.31
N4781.....	7 SB T	22.5	<8.19	0.60	1	...	<0.07
N4793.....	5 SX T	38.9	8.53	1.04	1	...	0.05

TABLE 1—*Continued*

Name	Type	D (Mpc)	log $L_N(L_\odot)$	A (kpc)	Reference	Class	C
N4808.....	6 SA S	20.9	<8.02	0.56	1	...	<0.06
N4818.....	2 SX T	21.5	9.30	0.57	1	...	0.95
N4826.....	2 SA T	4.1	7.15	0.12	11	L	0.05
N4845.....	2 SA S	15.6	8.41	0.42	1	...	0.34
N4861.....	9 SB S	17.8	<7.88	0.47	10	H INT	...
N4900.....	5 SB T	17.3	<8.00	0.46	1	...	<0.11
N4899.....	5 SX T	38.4	<8.45	1.02	1	H	<0.16
N4902.....	3 SB R	39.2	<8.50	1.05	1	L	<0.06
N4945.....	6 SB S	5.2	8.43	0.25	19	L/S	0.07
N4981.....	4 SX R	27.8	8.41	0.74	1	...	0.11
N4984.....	−1 SX T	21.3	9.05	0.57	1	...	0.59
N4995.....	3 SX T	28.0	<8.40	0.75	1	L/H	<0.09
N5005.....	4 SX T	21.3	8.66	0.57	1	L	0.09
N5053.....	5 SA S	18.7	<7.95	0.50	1	L	<0.02
N5055.....	4 SA T	7.2	<7.03	0.21	11	L	<0.01
N5054.....	4 SA S	27.3	8.61	0.73	1	H	0.14
N5085.....	5 SA S	28.9	8.38	0.77	1	...	0.06
N5188.....	3 SX S	32.9	9.26	0.88	1	H	0.42
N5194.....	4 SA S	7.7	7.38	0.30	20	L INT	0.01
N5195.....	90	9.3	8.47	0.38	21	L INT	0.47
N5236.....	5 SX S	4.7	7.56	0.13	11	H	0.01
N5247.....	4 SA S	22.2	<7.98	0.59	1	H	<0.02
N5297.....	5 SX S	37.8	<8.56	1.01	1	INT	...
N5301.....	4 SA S	27.7	<8.29	0.74	1	H	<0.08
N5350.....	3 SB R	37.8	8.74	1.01	1	L INT	...
N5371.....	4 SX T	37.8	<8.47	1.01	1	L	<0.04
N5383.....	3 SB T	37.8	8.67	1.01	1	...	0.18
N5427.....	5 SA S	38.1	8.68	1.02	1	S2 INT	0.04
N5457.....	6 SX T	4.7	6.71	0.13	11	H INT	0.01
N5480.....	5 SA S	31.9	8.44	0.85	1	H INT	0.16
Circinus.....	3 SA S	4.2	9.05	0.20	19	L/S	0.63
N5506.....	1	28.7	9.63	0.70	22	S2 INT	0.75
N5595.....	5 SX T	38.5	<8.74	1.03	1	H INT	<0.09
N5597.....	6 SX S	38.6	8.92	1.03	1	H INT	0.18
N5633.....	3 SA T	37.1	<8.52	0.99	1	...	<0.12
N5660.....	5 SX T	37.2	8.64	0.99	1	...	0.14
N5665.....	5 SX T	35.4	8.49	0.94	1	INT	0.10
N5668.....	7 SA S	26.9	<8.14	0.72	1	...	<0.17
N5678.....	3 SX S	35.6	8.84	0.95	1	INT	0.09
N5676.....	4 SA T	34.5	<8.51	0.92	1	L	<0.04
N5740.....	3 SX T	26.6	8.05	0.71	1	INT	<0.06
N5757.....	3 SB R	39.5	9.13	1.05	1	H	0.16
N5775.....	5 SB	26.7	8.23	0.71	1	H INT	0.02
N5806.....	3 SX S	28.5	<8.29	0.76	1	...	<0.10
N5861.....	5 SX T	28.9	<8.33	0.77	1	...	<0.05
N5921.....	4 SB R	25.2	<8.05	0.67	1	L	<0.05
N5929.....	2	38.5	<8.80	1.59	23	S2 INT	<0.18
N5954.....	6 SX T	32.1	8.22	0.90	17	H INT	...
N6221.....	5 SB S	19.4	8.94	0.71	24	S2	0.29
N6384.....	4 SX R	26.6	<7.90	0.76	11	L	...
N6764.....	4 SB S	37.0	9.22	1.02	25	L/H	0.58
N6814.....	4 SX T	22.8	8.37	0.63	25	S1	0.21
N6946.....	6 SX T	5.5	8.32	0.36	26	H	0.09
N7172.....	1	33.9	9.11	0.82	22	S2	0.38
N7213.....	1 SA S	22.0	9.00	0.80	24	S1	0.49
N7331.....	3 SA S	14.3	<8.08	0.40	2	L	<0.03
N7448.....	4 SA T	30.3	<8.42	0.81	1	H	<0.09
N7479.....	5 SB S	32.4	9.41	0.86	1	L	0.30
N7497.....	7 SB S	24.1	<8.49	0.64	1	...	<0.23
N7541.....	4 SB T	33.4	8.86	0.89	1	H	0.07
N7552.....	2 SB S	19.5	9.74	1.19	1	L/H INT	0.92
N7582.....	2 SB S	17.6	9.39	1.00	1	S2	1.
N7625.....	1 SA T	23.0	8.47	0.61	1	H INT	0.15
N7714.....	3 SB S	36.9	9.49	0.98	1	H INT	1.
N7721.....	5 SA S	26.1	<8.54	0.70	1	H	<0.28
N7723.....	3 SB R	23.7	<8.37	0.63	1	H	<0.15
N7793.....	7 SA S	2.8	<6.60	0.08	2	...	<0.05

REFERENCES.—1: Devereux 1987; 2: Rieke & Lebofsky 1978; 3: Rieke & Low 1975; 4: Lonsdale et al. 1984; 5: as quoted in Condon et al. 1982; 6: Ho et al. 1989; 7: Telesco & Gatley 1981; 8: Becklin et al. 1980; 9: Frogel et al. 1982; 10: Devereux et al. 1987; 11: Cizdziel et al. 1985; 12: Wright et al. 1988; 13: Lawrence et al. 1985; 14: Rieke et al. 1980; 15: Rieke & Low 1972; 16: Graham et al. 1984; 17: Cutri & McAlary 1985; 18: Willner et al. 1985; 19: Moorwood & Glass 1984; 20: Telesco et al. 1986; 21: Lebofsky & Rieke 1979; 22: Ward et al. 1987; 23: Edelson et al. 1987; 24: Glass et al. 1982; 25: Rieke 1978; 26: Rieke 1976.

distortion or structural peculiarity). Disturbed galaxies with no apparent companions tend to be unrecognized as interacting (see, e.g., the case of Maffei 2 discussed by Hurt et al. 1993). It is not easy to understand whether this bias (which is common to most statistical studies on the effects of galaxy interactions) can affect significantly the results, since we would need to have a (presently unavailable) wide sample of interacting galaxies which are selected solely on the basis of the presence of morphological features unmistakeably associated with a certain range of tidal strengths.

We have taken the *IRAS* 25 and 12 μm fluxes directly (in order of preference) from the papers of Soifer et al. (1989), Helou et al. (1988), Rice et al. (1988), and Devereux (1987), which generally report global co-added fluxes from all *IRAS* survey data, and from the Cataloged Galaxies and Quasars Observed in the *IRAS* Survey (Fullmer & Lonsdale 1989), which generally reports point source fluxes; for NGC 4151 we have used the *IRAS* pointed observations of Edelson & Malkan (1987).

Our sample, which is the most extensive—albeit not complete—set of small-beam MIR photometric data so far examined in the literature, can be regarded as representative of the 10 μm luminosity of the central regions (of $\sim$0.5–1 kpc, typically) of nearby spirals. The inhomogeneity of our data set is limited by the fact that about half of it comes directly from the photometric survey of Devereux (1987) alone. We purposely avoid choosing galaxies by virtue of some unusual property (e.g., infrared-bright galaxies, peculiar and interacting galaxies, galaxies with active or starburst nuclei). Therefore, our galaxy sample is less biased toward infrared bright galaxies and, in general, toward exceptionally bright (in the optical and infrared spectral bands) objects than several samples used in previous MIR studies (cf. the infrared-selected galaxy samples of Devereux 1987, Carico et al. 1988, Wright et al. 1988). Yet our sample is likely to be still a little biased in that sense (compared to a hypothetical complete sample), simply because the attention of many observers was focused on those objects. This bias implies that Seyfert galaxies (8%) and interacting objects (29%) are overrepresented in our sample; it also probably leads to a general underestimation of the number of nuclei of low 10 μm luminosity, although it should not affect relative comparisons between the various categories of objects.

3. STATISTICAL ANALYSIS

Owing to the fairly large number of upper limits on the MIR flux densities, we have made use of statistical techniques suitable for the analysis of censored data and adapted to astronomical usage from the field of survival analysis (see, e.g., Schmitt 1985; Feigelson & Nelson 1985; Isobe, Feigelson, & Nelson 1986; for extensive discussions on the astronomical applications). If the nondetected galaxies were dropped from the sample (as was done in previous efforts to characterize the typical MIR luminosities of galactic nuclei), the resulting sample would be skewed toward infrared-bright galaxies in a complicated fashion that depends on the MIR luminosity function and on the sensitivity limits. In practice, we have used the software package ASURV (Rev 1.0) (Isobe & Feigelson 1990) which was kindly provided to us by E. Feigelson.

We have employed the Kaplan-Meier product-limit estimator in order to calculate the means, medians, and cumulative distribution functions of the quantity log L_N for various subsets of galaxies. The Kaplan-Meier estimator, which is the cornerstone of the nonparametric survival analysis, had been proved to be the unique self-consistent, generalized maximum-likelihood, asymptotically normal estimator (under quite broad conditions) of the empirical distribution functions of a randomly censored data set. The estimated cumulative distribution function (though not the associated errors) is identical to the iterative solution derived by Avni et al. (1980); it is a piecewise continuous and piecewise constant function with jumps at the uncensored (detected) values. The Kaplan-Meier estimator adequately treats detections and redistributes upper limits, recovering the information lost by censoring; it has been shown to be valid under quite diverse conditions (Feigelson & Nelson 1985). The median of the distribution function is always well defined. If the lowest point in the sample is an upper limit, the mean is not well defined, since the distribution is not normalizable, and so the outlying censored point is redefined as a detection in our analysis.

The comparison of the distribution functions of log L_N of pairs of subsamples is accomplished by using two versions of Gehan's test (one with permutation variance and the other with hypergeometric variance), the logrank, the Peto-Peto, and the Peto-Prentice tests. These tests differ in how the censored points are weighted and consequently have different sensitivities and efficiencies with different distributions and censoring patterns.

The 10 μm emission of many galaxies is characterized by an appreciable spatial extent ($>$0.5 kpc), as was stressed by the high-resolution 10 μm maps of Ho et al. (1989) and by the small-beam 10 μm photometry of Devereux (1987), Wright et al. (1988), Carico et al. (1988), Hill et al. (1988), which is frequently compared with the large-beam *IRAS* 12 μm fluxes. Thus, log L_N is expected to increase as the beam diameter A (in kpc) grows. This is illustrated by the log L_N–log A plot (Fig. 1). Figure 1 shows that log L_N increases approximately linearly with log A up to $A \sim 1$ kpc (which can be taken as a typical lower limit for the spatial extension of the 10 μm emission). In order to calculate the linear regression line in this case, in which upper limits on the independent variable are present, we have used three methods: the EM algorithm, which requires that the functional form of the distribution of the dependent variable about the regression line be specified (a normal distribution is generally assumed); the nonparametric EM algorithm with Kaplan-Meier estimator, suggested by Buckley & James (1979); and Schmitt's method (see, e.g., Isobe et al. 1986). All three methods concur that the slope of the log L_N–log A relation is 1.7 ± 0.2, that is, close to 2 (the value typical for a constant surface brightness source). More specifically, these considerations hold for the non-Seyfert objects, since the 23 Seyfert galaxies exhibit no significant log L_N–log A correlation. This would suggest that the MIR emission of Seyfert galaxies is not so extended as that of the other galaxies. This issue will be better addressed below in the discussion of the compactness parameter C. In the comparison of the log L_N distributions of pairs of galaxy subsamples, one should take into account the bias due to the log L_N–log A relation by comparing subsamples having a similar range of A-values. In practice, we deem it enough to exclude objects with $A < 0.3$ kpc in order to minimize this bias.

As expected, the compactness parameter C shows a tendency to increase with growing A. The C-A plot is shown in Figure 2; in this figure the dashed lines represent a grid of simple galaxy models in which the surface brightness decreases as e^{-r/r_s}, where r_s is the characteristic radius of the surface brightness distribution. This plot is similar to that introduced by Hill et al.

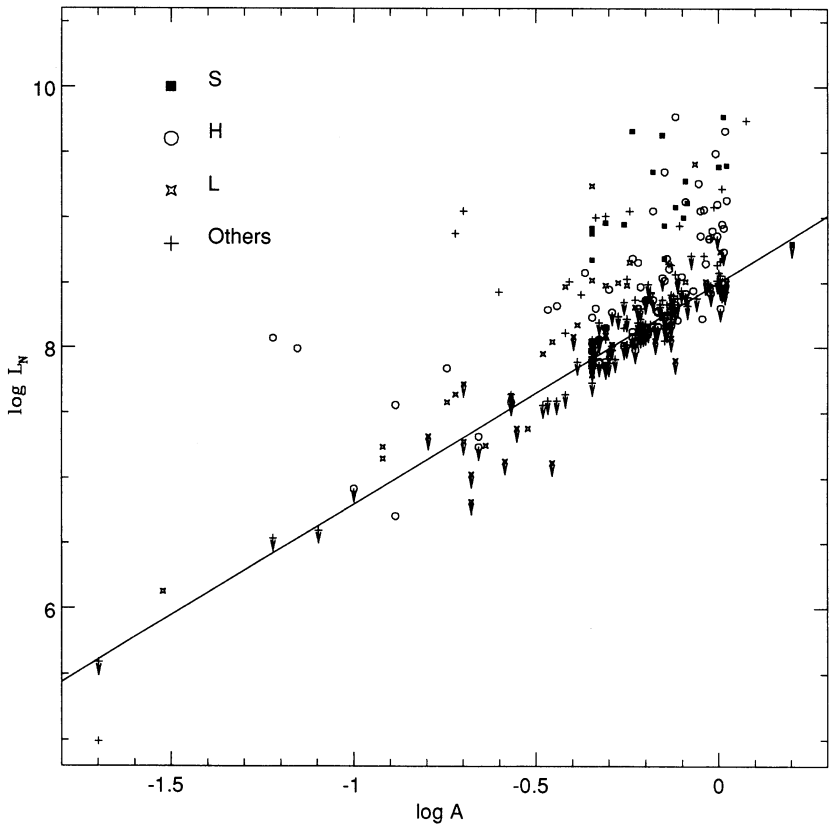

FIG. 1.—The log L_N–log A plot, where the 10 μm luminosity L_N is in solar units and the projected diameter A of the central region is in kiloparsecs. Different symbols denote the Seyfert galaxies, the H II region–like nuclei, the LINERs, and the other objects. Upper limits on L_N are denoted by arrows. The solid line is the mean linear regression line.

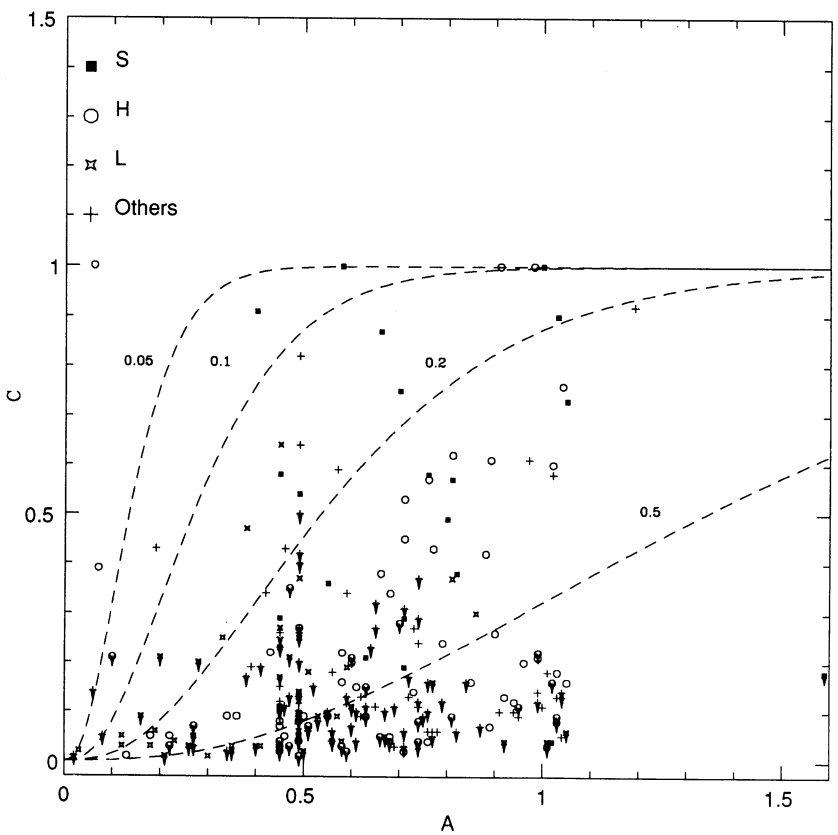

FIG. 2.—The C-A plot, where C is the compactness parameter. Symbols as in Fig. 1. The dashed lines represent a grid of simple galaxy models in which the surface brightness decreases as e^{-r/r_s}, where r_s is the characteristic radius (in kiloparsecs) of the surface brightness disribution of the galaxy.

(1988), except that in this case we are plotting aperture diameters instead of distances. Seyfert galaxies are characterized by smaller scale sizes (r_s) than the norm; most objects cluster around scale size $\gtrsim 0.5$ kpc. Also in the analysis of the C-distributions, we shall exclude the objects with $A < 0.3$ kpc.

We define the MIR central surface brightness as $S_N = L_N/A^2$ (where S_N is expressed in units of solar luminosity per square kpc). The quantity log S_N exhibits no significant correlation with A (see the log S_N–log A plot illustrated in Figure 3), which is consistent with the fact that the 10 μm emission is generally extended. We have verified the absence of correlation by computing the correlation probabilities based on the Cox proportional hazard model, on the generalized Kendall rank correlation statistics, and on the generalized Spearman rank order correlation coefficient. For $N_T = 281$ objects with $N_L = 137$ upper limits on log S_N we have found high probabilities that the two variables log S_N and log A are independent ($p = 0.47, 0.89, 0.79$, for the three respective tests). Therefore, in comparing the log S_N distributions of pairs of galaxy samples we shall consider all objects irrespective of their A-values.

The compactness parameter C shows a moderate correlation with log L_N and log S_N (see Figs. 4 and 5). This is essentially due to the fact that the brightest categories of nuclei (at MIR wavelengths)—such as Seyfert galaxies, H II nuclei, and interacting nuclei—tend to have also more compact emission than the norm. (This is discussed in detail in the following section.)

For various subsamples Table 2 contains the main result of our statistical analysis: the total number N_T of (detected and undetected) objects; the number N_L of upper limits (undetected galaxies); the estimated medians, means, and standard deviations σ of the distribution functions of log L_N (for $A \geq 0.3$ kpc); log S_N (for all values of A); C (for $A \geq 0.3$ kpc). Table 3 gives the numerical outcomes from the comparison of the distributions of many pairs of galaxy subsamples, namely the (two-tailed) probabilities p that two data subsets come from the same underlying population. In Table 3 we give the mean [p(mean)], minimum [p(min)], and maximum [p(max)] values of the five probabilities coming out from the application of the five above-mentioned tests. The statistical significance of the difference between the distributions of two data subsets is at the $100\cdot(1 - p)\%$ level. These five tests give somewhat different results especially when the data set is small or suffers from heavy censoring.

The main results which can be inferred from an inspection of Tables 2 and 3 are discussed below. In all tables L_N is expressed in units of solar luminosity and S_N in units of solar luminosity per square kpc.

4. RESULTS AND DISCUSSION

4.1. *Seyfert and Non-Seyfert Galaxies*

First of all, it is very clear that the Seyfert nuclei (denoted by S in the tables) are unequivocally the most powerful MIR sources, since they have typically greater 10 μm luminosities and surface brightnesses than the non-Seyfert ones (NON-S) (from which we have excluded the objects classed as L/S in order to be conservative). Seyfert galaxies are also intrinsically brighter at 10 μm than the two individual classes of H II region–like (H) and LINER (L) nuclei. Our new finding, which indicates an excess MIR emission of Seyfert galaxies with

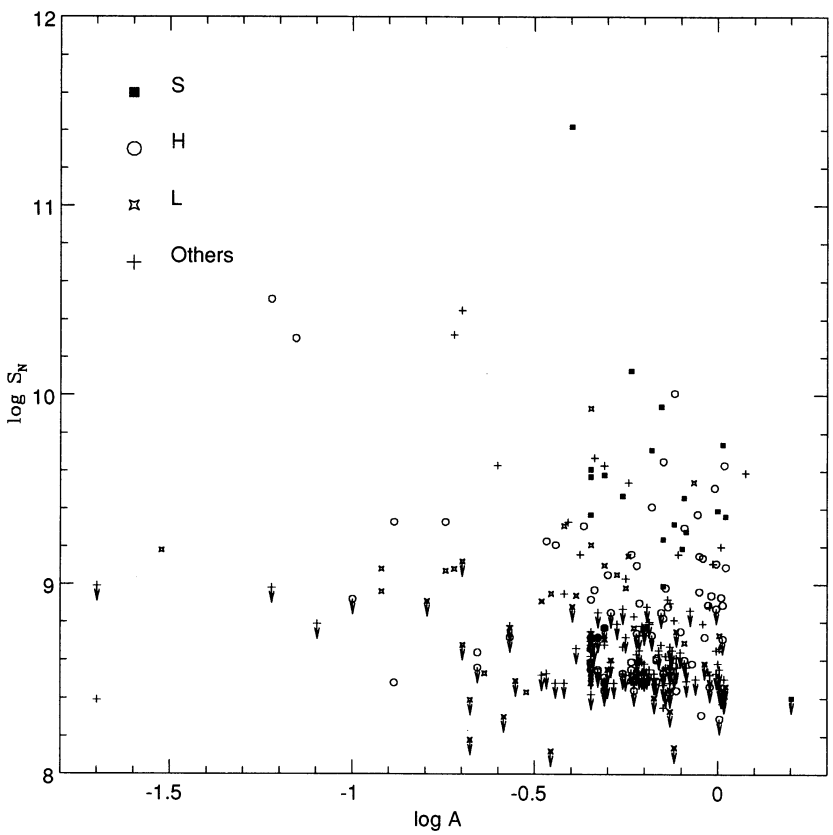

FIG. 3.—The log S_N–log A plot, where S_N is the 10 μm surface brightness (in $L_\odot$ kpc^{-2}). Symbols as in Fig. 1.

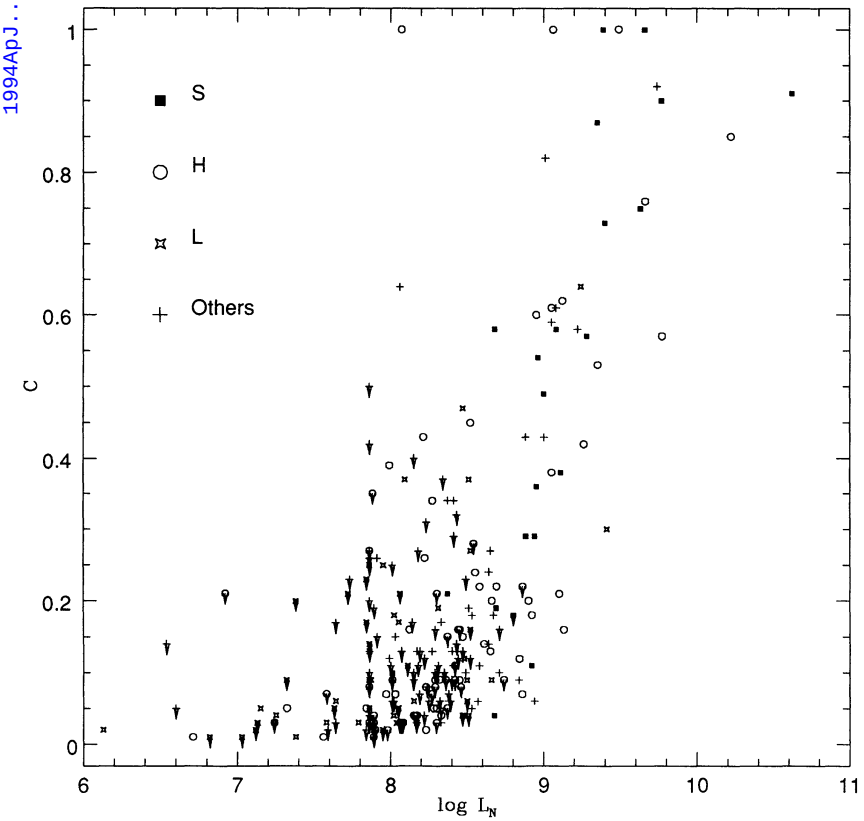

FIG. 4.—The C–log L_N plot. Symbols as in Fig. 1.

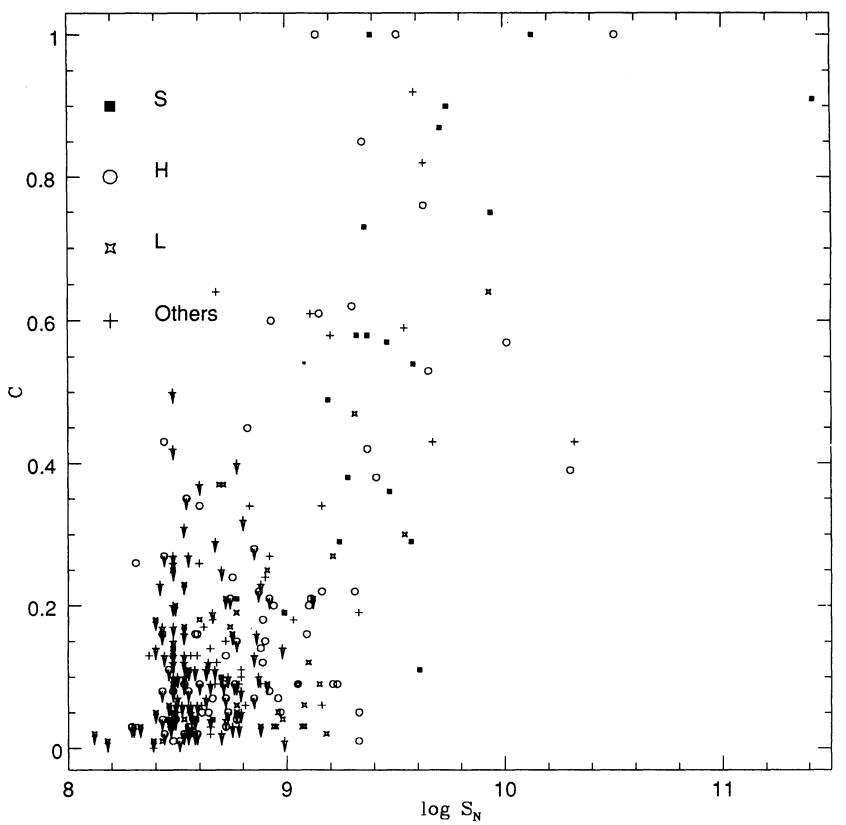

FIG. 5.—The C–log S_N plot. Symbols as in Fig. 1.

TABLE 2

MEDIANS, MEANS, AND STANDARD DEVIATIONS

Subsample	Variable	NT	NL	Median	Mean	σ
S	$\log L_N$	23	3	8.96	9.03	0.12
S	$\log S_N$	23	3	9.37	9.38	0.13
S	C	22	2	0.49	0.49	0.07
NON-S	$\log L_N$	226	120	8.01	8.01	0.06
NON-S	$\log S_N$	255	135	8.48	8.60	0.03
NON-S	C	192	98	0.09	0.14	0.02
H	$\log L_N$	72	29	8.62	8.40	0.07
H	$\log S_N$	81	32	8.63	8.77	0.06
H	C	64	26	0.06	0.18	0.03
L	$\log L_N$	44	22	7.90	7.94	0.10
L	$\log S_N$	58	30	8.47	8.55	0.06
L	C	37	18	0.03	0.11	0.02
UNC	$\log L_N$	110	69	7.92	7.99	0.05
UNC	$\log S_N$	116	73	8.38	8.57	0.03
UNC	C	91	54	0.12	0.13	0.02
EARLY	$\log L_N$	87	37	8.05	8.13	0.09
EARLY	$\log S_N$	100	42	8.60	8.69	0.05
EARLY	C	75	30	0.19	0.21	0.03
LATE	$\log L_N$	135	81	7.83	7.91	0.06
LATE	$\log S_N$	152	91	8.41	8.53	0.04
LATE	C	113	66	0.07	0.08	0.01
INT	$\log L_N$	58	20	8.23	8.24	0.10
INT	$\log S_N$	66	22	8.60	8.77	0.06
INT	C	44	16	0.17	0.23	0.04
NON-INT	$\log L_N$	168	100	7.96	7.92	0.07
NON-INT	$\log S_N$	189	113	8.38	8.52	0.04
NON-INT	C	148	82	0.08	0.11	0.01
INT (L)	$\log L_N$	13	3	8.07	8.07	0.13
INT (L)	$\log S_N$	17	4	8.72	8.79	0.07
INT (L)	C	10	3	0.09	0.16	0.05
NON-INT (L)	$\log L_N$	31	19	7.70	7.88	0.15
NON-INT (L)	$\log S_N$	41	26	7.04	8.45	0.07
NON-INT (L)	C	27	15	0.02	0.09	0.03
INT (H)	$\log L_N$	29	8	8.55	8.57	0.12
INT (H)	$\log S_N$	32	9	8.61	8.85	0.10
INT (H)	C	22	5	0.21	0.31	0.07
NON-INT (H)	$\log L_N$	43	21	8.32	8.28	0.07
NON-INT (H)	$\log S_N$	49	23	8.64	8.72	0.07
NON-INT (H)	C	42	21	0.05	0.11	0.02
INT (H + LATE)	$\log L_N$	39	16	8.24	8.33	0.12
INT (H + LATE)	$\log S_N$	42	17	8.54	8.74	0.08
NONINT (H + LATE)	$\log L_N$	76	45	7.99	8.04	0.07
NON-INT (H + LATE)	$\log S_N$	86	51	8.27	8.59	0.04
SA	$\log L_N$	71	44	7.78	7.79	0.08
SA	$\log S_N$	82	50	8.40	8.52	0.05
SA	C	62	38	0.07	0.07	0.01
SB	$\log L_N$	68	33	8.04	8.19	0.08
SB	$\log S_N$	72	35	8.59	8.70	0.05
SB	C	55	23	0.08	0.23	0.04
SB + SX	$\log L_N$	148	72	8.05	8.19	0.05
SB + SX	$\log S_N$	165	80	8.54	8.64	0.04
SB + SX	C	123	55	0.11	0.17	0.02
SA T = 3, 4, 5	$\log L_N$	50	33	7.37	7.75	0.09
SA T = 3, 4, 5	$\log S_N$	56	37	8.39	8.49	0.06
SA T = 3, 4, 5	C	46	31	0.06	0.05	0.01
SB T = 3, 4, 5	$\log L_N$	36	17	8.63	8.37	0.09
SB T = 3, 4, 5	$\log S_N$	37	17	8.65	8.72	0.06
SB T = 3, 4, 5	C	31	13	0.07	0.18	0.05
SB + SX T = 3, 4, 5	$\log L_N$	91	50	8.05	8.25	0.05
SB + SX T = 3, 4, 5	$\log S_N$	102	54	8.45	8.59	0.05
SB + SX T = 3, 4, 5	C	78	38	0.09	0.14	0.03
SA (NON-H)	$\log L_N$	51	33	7.41	7.75	0.09
SA (NON-H)	$\log S_N$	62	40	8.39	8.50	0.06
SB (NON-H)	$\log L_N$	46	27	7.64	8.04	0.09
SB (NON-H)	$\log S_N$	48	28	7.46	8.63	0.06
SA (NON-L)	$\log L_N$	56	34	7.98	7.98	0.06
SA (NON-L)	$\log S_N$	60	37	8.38	8.54	0.03
SB (NON-L)	$\log L_N$	54	25	8.10	8.24	0.09
SB (NON-L)	$\log S_N$	57	26	8.61	8.70	0.06
SA (NON-INT)	$\log L_N$	57	39	7.05	7.69	0.09
SA (NON-INT)	$\log S_N$	67	45	8.38	8.48	0.06
SB (NON-INT)	$\log L_N$	49	28	7.68	8.08	0.09
SB (NON-INT)	$\log S_N$	59	29	7.90	8.64	0.05
SR	$\log L_N$	25	16	7.47	7.79	0.14
SR	$\log S_N$	28	17	7.37	8.46	0.08
ST + SS	$\log L_N$	182	95	8.03	8.05	0.06
ST + SS	$\log S_N$	207	109	8.47	8.61	0.03

TABLE 3

STATISTICAL COMPARISONS

Subsamples	Variable	p(mean)	p(min)	p(max)
S/NON-S	log L_N	<0.0001	<0.0001	<0.0001
S/NON-S	log S_N	<0.0001	<0.0001	<0.0001
S/NON-S	C	<0.0001	<0.0001	<0.0001
S/H	log L_N	<0.0001	<0.0001	<0.0001
S/H	log S_N	<0.0001	<0.0001	<0.0001
S/H	C	<0.0001	<0.0001	<0.0001
S/L	log L_N	<0.0001	<0.0001	<0.0001
S/L	log S_N	<0.0001	<0.0001	<0.0001
S/L	C	<0.0001	<0.0001	<0.0001
H/UNC	log L_N	0.0007	0.0005	0.0008
H/UNC	log S_N	0.0003	0.0001	0.0007
H/UNC	C	0.22	0.18	0.33
L/UNC	log L_N	0.92	0.85	1.00
L/UNC	log S_N	0.19	0.10	0.36
L/UNC	C	0.67	0.59	0.73
L/H	log L_N	0.005	0.004	0.008
L/H	log S_N	0.07	0.06	0.08
L/H	C	0.20	0.15	0.24
EARLY/LATE	log L_N	0.03	0.03	0.05
EARLY/LATE	log S_N	0.003	0.002	0.005
EARLY/LATE	C	<0.0001	<0.0001	0.0002
INT/NON-INT	log L_N	0.004	0.002	0.006
INT/NON-INT	log S_N	0.004	0.001	0.006
INT/NON-INT	C	0.009	0.005	0.016
INT/NON-INT (L)	log L_N	0.12	0.09	0.13
INT/NON-INT (L)	log S_N	0.018	0.005	0.027
INT/NON-INT (L)	C	0.06	0.02	0.09
INT/NON-INT (H)	log L_N	0.09	0.07	0.13
INT/NON-INT (H)	log S_N	0.44	0.36	0.49
INT/NON-INT (H)	C	0.03	0.01	0.06
INT/NON-INT (H + LATE)	log L_N	0.04	0.02	0.08
INT/NON-INT (H + LATE)	log S_N	0.25	0.23	0.28
SA/SB	log L_N	0.011	0.002	0.034
SA/SB	log S_N	0.017	0.007	0.043
SA/SB	C	0.0004	<0.0001	0.0005
SA/SB + SX	log L_N	0.004	0.001	0.010
SA/SB + SX	log S_N	0.016	0.007	0.043
SA/SB + SX	C	0.003	<0.001	0.007
SA/SB T = 3, 4, 5	log L_N	0.002	0.001	0.005
SA/SB T = 3, 4, 5	log S_N	0.003	0.001	0.005
SA/SB T = 3, 4, 5	C	0.0013	0.0004	0.0022
SA/SB + SX T = 3, 4, 5	log L_N	0.010	0.004	0.025
SA/SB + SX T = 3, 4, 5	log S_N	0.025	0.006	0.071
SA/SB + SX T = 3, 4, 5	C	0.006	0.003	0.008
SA/SB (NON-H)	log L_N	0.23	0.14	0.41
SA/SB (NON-H)	log S_N	0.16	0.09	0.30
SA/SB (NON-L)	log L_N	0.032	0.008	0.096
SA/SB (NON-L)	log S_N	0.016	0.008	0.039
SA/SB (NON-INT)	log L_N	0.04	0.01	0.11
SA/SB (NON-INT)	log S_N	0.04	0.02	0.09
SR/ST + SS	log L_N	0.23	0.20	0.28
SR/ST + SS	log S_N	0.57	0.45	0.69

respect to non-Seyfert galaxies, appears to be consistent with the results of Spinoglio & Malkan's (1989) study of an extensive 12 μm flux-limited sample of *IRAS* sources. Emphasizing the use of the *IRAS* 12 μm flux as a good index of nonstellar emission and as a powerful technique of AGN selection, the two authors found that Seyfert galaxies have, on average, higher 12 μm luminosities than non-Seyfert galaxies. Our analysis provides decisive proof of the predominance of Seyfert galaxies in the MIR emission, since *IRAS* beams, being about a few arcminutes in size, encompass a substantial fraction of the entire galaxy (except in very nearby objects) and are thus less appropriate to the study of galactic nuclear emission.

Seyfert galaxies are characterized by a much more compact MIR emission than the other categories of objects, although in many (15) Seyfert galaxies (68%) the compactness parameter C is low enough ($C < 0.7$) to indicate the presence of a substantial extended emission. This result is not appreciably affected by the possible presence of a 9.7 μm absorption silicate feature, which would suppress the ground-based 10 μm flux proportionally more than the *IRAS* 12 μm flux (because of the wider bandpass of the *IRAS* 12 μm filter). Hill et al. (1988) have evaluated the amount of the consequent reduction of the compactness parameter C for a different spectral index of the power-law continuum of the source and different optical depth at 9.7 μm. According to their calculations, for a quite negative spectral index (i.e., $F_\nu \propto \nu^n$ with $n = -2$), the effect is a 13% and 24% decrease of C for $\tau_{9.7\mu m} = 1$ and 2, respectively (greater spectral indices lead to smaller effects). The observa-

tions of the MIR spectra of galactic nuclei show that most of the galaxies having this silicate absorption band, which is thought to arise in dusty regions fairly close to the central source, are type 2 Seyfert galaxies (Roche et al. 1991), for which $\tau_{9.7\,\mu m} < 2$ is a typical value (e.g., Roche et al. 1984). Even if we hypothesize an underestimation of the parameter C by 25% for all the Seyfert galaxies of our sample which are not classed as Seyfert 1 galaxies, we still find 13 objects (59%) with fairly low C ($C < 0.7$). This indicates that extended thermal MIR emission from dust warmed by hot stars in the outer regions (beyond ~ 0.5 kpc from the center) is important in the majority of Seyfert galaxies, in agreement with the abundance of H II regions (in the galactic disks) which are observed in optical emission-line surveys (e.g., Pogge 1989).

Interestingly, both the subset of far-infrared luminous galaxies (of the *IRAS* Bright Galaxy sample) observed by Carico et al. (1988) in the near- and mid-infrared and the sample of 19 *IRAS* luminous galaxies, observed by Wynn-Williams & Becklin (1993) in several MIR bands, exhibit, on average, somewhat more compact 10 μm emission than our sample of Seyfert galaxies. According to Carico et al. (1988), who compared their own small-beam 10 μm measures with the *IRAS* 12 μm fluxes, half of these galaxies have 10 μm emission consistent with a contribution of 50% or more from a central point source. Wynn-Williams & Becklin (1993), who measured directly the compactness at $\lambda \sim 12$ μm and $\lambda \sim 25$ μm through observations made with filters centered just at these two wavelengths, found $C \geq 0.5$ for all galaxies (at both wavelengths). The great compactness of the MIR emission of these infrared bright galaxies may be related to their particularly great infrared luminosities, with which the degree of compactness is found to correlate (Carico et al. 1988).

The great predominance of Seyfert galaxies in MIR emission is consistent with their well-known strong predominance in near-infrared emission (e.g., Glass & Moorwood 1985), in radio continuum emission (e.g., Ulvestad, Wilson, & Sramek 1981; Giuricin, Mardirossian, & Mezzetti 1988b), and in soft X-ray emission (e.g., Kriss, Canizares, & Ricker 1980, and Giuricin et al. 1991 for Seyfert types 1 and 2 galaxies, respectively). Furthermore, the *IRAS* data indicate that the Markarian Seyfert galaxies exhibit also an excess of 25 μm flux with respect to the Markarian starbursts galaxies (Hunt 1991). On the contrary, the far-infrared luminosities of these two classes of objects are similar (Rodriguez-Espinosa, Rudy, & Jones 1987; Dahari & De Robertis 1988).

4.2. *Interacting and Noninteracting Galaxies*

Among the non-Seyfert galaxies from which we have excluded the objects classed as L/S) the interacting objects (denoted by INT in the tables) exhibit greater values of L_N and S_N in general than the noninteracting (NON-INT) galaxies, in qualitative agreement with earlier results (Lonsdale et al. 1984; Cutri & McAlary 1985; Wright et al. 1988). However, these studies tend to be biased toward the most extreme cases of strong interactions and do not properly include the upper limits in their analysis; therefore, they tend to overestimate the L_N differences between the interacting and noninteracting galaxies. For instance, Wright et al. (1988) reported a ratio of greater than 10 between the L_N averages of the two categories, while our Table 2 gives a ratio of ~ 2 only (~ 1.7 for the S_N averages).

In addition, we are able to explore the effects of interactions on the intensity of the MIR emission separately for the two classes of LINER and H II region–like nuclei. Tables 2 and 3 reveal that the difference between the interacting and noninteracting LINERs [denoted by INT (L) and NON-INT (L), respectively] is considerable in the case of the S_N distributions (it is small in the case of the L_N distributions for $A \geq 0.3$ kpc, because of poor statistics). On the other side, the interacting and noninteracting H II nuclei [denoted by INT (H) and NON-INT (H)] differ very little in the L_N distributions and not at all in the S_N. We have verified that the reason for this behavior of the H II nuclei stems from the fact that the L_N-values of the interacting H II nuclei generally refer to greater A-values than the noninteracting do. (The median values of A are 0.71 kpc and 0.60 kpc, respectively.) On the reasonable hypothesis that a discrete number of the unclassified nuclei hosted in late-type spirals are likely to be H II nuclei, we have tried to improve the statistics by adding to our sample of H II nuclei all unclassified galaxies of type Sc and later. This enlarged data sample confirms the marginal difference between the L_N distributions of the interacting and noninteracting objects [denoted by INT (H + LATE) and NON-INT (H + LATE), respectively, in Tables 2 and 3] and the absence of difference in the S_N distributions. Hence, some interaction-induced enhancement of the MIR emission in H II nuclei may be caused by a spread of the MIR emission over a somewhat larger area (which may be due to an enlargement of starburst regions) rather than to an increase in the central MIR surface brightness, as occurs in the case of interacting LINERs. Notably, the difference in the interaction effects on the MIR emission of the two categories of nuclei bears considerable similarity with the interaction-induced enhancement of the central radio emission of LINER and H II nuclei (see Giuricin et al. 1990).

Interacting objects also exhibit more compact MIR emission than noninteracting ones. This holds for both H II and LINER nuclei. This finding specifies that the interaction-induced enhancement of the MIR emission concerns preferentially the central galactic regions rather than the outer disk regions (as first suspected by Lonsdale et al. 1984), although the compactness parameter C is great ($C > 0.5$) only in eight (18%) interacting objects.

The increased compactness of the 10 μm emission of interacting objects agrees with the similar behavior of various indices of star formation activity: Hα line emission (Bushouse 1987), radio emission (Hummel 1981b; Condon et al. 1982), far-infrared emission (Bushouse 1987), and near-infrared emission (Joseph et al. 1984; Cutri & McAlary 1985); in the latter case the effect was found to be detectable in H II nuclei only (Giuricin et al. 1993). All these results are generally taken as an indication that current star formation activity (induced by interactions) preferentially occurs in and near the nuclear regions of galaxies rather than in their outer disk regions (see also Laurikanien & Moles 1989 and the review by Heckman 1990).

4.3. H II *Region–like and LINER Nuclei*

The H II nuclei tend to display greater values of L_N and S_N than the extensive sample of the unclassified nuclei (denoted by UNC in Tables 2 and 3), which also comprises the few objects classed as L/H and T. On the other hand, the LINERs have L_N and S_N distributions similar to those of the unclassified nuclei. In agreement with these results, a straightforward comparison between the H II and LINER nuclei reveals that the former category has typically greater values of L_N and S_N than the

latter. This holds also for the two respective subsets of noninteracting objects alone.

Our results suggest that the MIR luminosity of LINERs is indistinguishable from that of normal (emission-line free) nuclei (which probably dominate the category of unclassified nuclei), in disagreement with the contention of Willner et al. (1985), who claimed that LINERs are more luminous than normal at ~ 10 μm on the basis of fewer objects. Furthermore, our results indicate that the starburst phenomenon leads to an appreciable increase in MIR emission, although the effect is certainly smaller than that related to Seyfert galaxies.

Unlike some previous contentions (Devereux 1987), the MIR emission of H II nuclei does not turn out to be typically more compact than that of LINER and unclassified objects. (Table 3 shows that the C distributions of these three categories of objects do not differ significantly.)

Interestingly, a specific comparison between H II nuclei and LINER nuclei leads to a strong difference in the same sense for radio continuum luminosities (Giuricin, Mardirossian, & Mezzetti, 1988a, b) and for the sizes of their central radio sources (Giuricin et al. 1990; Hummel et al. 1990). It also leads to a weak difference in the opposite sense for the near-infrared luminosities (in the J, H, K bands) of their central (~ 1 kpc diameter) (Giuricin et al. 1993). Furthermore, the near-infrared data of a sample of H II and LINER nuclei compiled by the latter authors show normal near-infrared colors (which are fully explainable in terms of emission from late-type evolved stars) for LINER nuclei, but strong redward deviations from the norm of the color indices $K - L$ of a subset of H II nuclei hosted in interacting galaxies. Redder near-infrared colors than normal are usual results of near-infrared photometric observations of far-infrared (*IRAS*)–bright galaxies (Moorwood, Véron-Cetty, & Glass 1986, 1987; Carico et al. 1986, 1988, 1990), of interacting galaxies (Joseph et al. 1984; Cutri & McAlary 1985; Lutz 1992); but there is as yet no consensus about the interpretation of this (as discussed in Giuricin et al. 1993). In the soft X-ray band (~ 0.5–4 keV) galaxies with H II and LINER nuclei exhibit emissions of comparable strengths (Giuricin et al. 1991).

4.4. *Early-Type and Late-Type Spirals*

Among the non-Seyfert galaxies, early-type spirals (Sb and earlier, denoted by EARLY in Tables 2 and 3) turn out to be slightly brighter at ~ 10 μm than late-type ones (Sbc and later, denoted by LATE in Tables 2 and 3) by an average factor of ~ 1.7 in L_N and ~ 1.4 in S_N; this occurs notwithstanding the preference of the H II nuclei to be hosted in late-type spirals, which would lead to the opposite tendency (and despite the comparable frequency of occurrence of interacting objects in the early and late morphological intervals). We have verified that the same tendency holds for the subsets of unbarred (or barred) galaxies alone (although its statistical significance becomes quite low because of poor statistics). This small tendency was already implicit in the data sample by Devereux et al. (1987) and Devereux (1987). This effect is certainly too large to be ascribed to a somewhat larger 10 μm flux contribution of bulge population stars, if this contribution is taken to be $\sim 10\%$ of the flux measured in the standard H band (at ~ 1.65 μm), according to the estimates of Impey, Wynn-Williams, & Becklin (1986) and the relevant discussion of Devereux et al. (1987).

Early-type spirals show much more compact emission than late-type ones. (We have verified that this tendency holds for all bar types.)

Owing to the negligible stellar emission at MIR wavelengths, our new finding cannot be a trivial result of the prominence of bulges in early-type spirals, which accounts for a similar difference in the central near-infrared luminosities of early- and late-type spirals (see, e.g., Devereux et al. 1987). Our finding is likely to be more closely linked with the results of the radio surveys of extensive samples of generic spiral galaxies. These reveal that early-type spirals contain stronger and more compact central radio sources than late-type objects (Hummel 1981a; van der Hulst, Crane, & Keel 1981). This difference is not confirmed in the recent study by Hummel et al. (1990), probably because their sample, being restricted to galaxies having LINER or H II nuclei, is skewed toward galaxies with H II nuclei (which are stronger radio sources than the norm and which occur mostly in late-type spirals). Incidentally, early-type spirals appear to have far-infrared luminosities similar to those of late-type ones (Isobe & Feigelson 1992).

4.5. *Barred and Unbarred Spirals*

Comparing the L_N distribution functions of barred and unbarred spirals via the Kolmogorov-Smirnov test (e.g., Hoel 1971), in which upper limits on L_N were replaced simply by detections, Devereux (1987) realized that barred spirals are typically brighter than unbarred ones in the early-type range (Sb and earlier), whereas no bar effect was observed in the latter types. Our survival analysis of non-Seyfert galaxies (classed as SA and SB) confirms the existence of this bar effect in the whole morphological sequence. However, trying several morphological type subdivisions, we have found that this bar effect is due essentially to the types Sb, Sbc, Sc (i.e., $T = 3, 4, 5$) at variance with the claims of Devereux (1987); as a matter of fact, we have verified that in other type intervals (such as $T < 3$, $T < 4$, $T < 5$, $T > 3$, $T > 4$, $T > 5$) this bar effect is weaker and sometimes statistically not significant. Including the transition bar-type SX into the category of barred (SB) galaxies, we have verified that unbarred spirals are fainter than SB + SX objects (in the whole morphological sequence and in the Sb, Sbc, Sc range). Interestingly, we have verified that this bar effect is no longer significant if we exclude the galaxies with H II nuclei from our sample [the two respective subsamples are denoted by SA (NON-H) and SB (NON-H) in Tables 2 and 3], while it becomes only a little less significant or almost equally significant if we exclude the interacting galaxies or the LINERs from our sample. This suggests that the association of bars with enhanced 10 μm emission holds mostly for H II nuclei.

The spatial distribution of the MIR emission appears to be more compact in barred galaxies (SB and SB + SAB) than in unbarred ones (SA) in the whole morphological range and in the types Sb, Sbc, Sc; again, as in our previous discussion on $\log L_N$ and $\log S_N$, we have verified that the bar effect on the compactness of the emission is substantially due to the types Sb, Sbc, Sc, in disagreement with Devereux (1987), who stressed the predominance of compact emission in the early types.

Analogously, barred spirals tend to have more powerful central radio sources than unbarred systems (Hummel 1981a); later, it was specified that this effect is substantially confined to galaxies with H II region–like nuclei only (Giuricin et al. 1990; Hummel et al. 1990), which is consistent with our results. No bar effect was found in the near-infrared colors $J - H$ and $H - K$ and in the near-infrared luminosities L_J, L_H, L_K of the central regions of non-Seyfert spirals (Giuricin et al. 1993). On the other hand, the studies of *IRAS* data have yielded discordant results. On the basis of a far-infrared–selected galaxy

sample, Hawarden et al. (1986) found that barred spirals (which do not host a LINER or Seyfert nucleus) have enhanced far-infrared luminosities as well as luminosity ratios $L_{25\mu m}/L_{12\mu m}$ and $L_{25\mu m}/L_{100\mu m}$ with respect to unbarred spirals. Bothun, Lonsdale, & Rice (1989) found similar far-infrared luminosities for optically selected barred and unbarred spirals. Last, analyzing a volume-limited sample of optically selected nearby spirals, Isobe & Feigelson (1992) claimed that barred spirals have, on average, fainter far-infrared luminosities than unbarred ones.

4.6. *Ringed and Unringed Spirals*

We have examined the effects of the ring types of the standard morphology classification reported in the RC3 catalog, comparing the L_N and S_N distributions of the S(r) spirals (which possess inner rings), the unringed S(s) spirals (with S-shaped arms), and the S(rs) (transition type) spirals (denoted, respectively, by SR, ST, SS in our Tables 2 and 3). No significant effect was found in the non-Seyfert nuclei (Tables 2 and 3 report some results).

Incidentally, Isobe & Feigelson (1992) claimed that $S(r)$ galaxies have weaker far-infrared luminosities than average.

4.7. *Relation between Radio and Mid-Infrared Emissions*

The results of our detailed comparison between the behavior of various categories of objects clearly emphasize that the 10 μm emission is particularly closely linked to the radio continuum emission, which in non-Seyfert galaxies is predominantly nonthermal synchrotron emission coming primarily from supernova remnants. Hence, our study, based on a wide sample of data, provides a meaningful, strong support for previous similar claims based on a detailed comparison of the MIR and radio maps of a few, well-observed galaxies (e.g., Telesco 1988; Ho et al. 1989), at resolution of several arcseconds (corresponding to several hundred parsecs); however, the MIR-radio correlation seems to become weaker at the smallest spatial scales (<100 pc) currently reachable at MIR wavelengths in very nearby galaxies (see, e.g., the high-resolution MIR maps of Telesco & Gezari 1992, and Piña et al. 1992 for M82 and N253, respectively). For non-AGNs the latter fact would favor mechanisms of thermal emission by small dust grains transiently heated radiatively by newly formed, hot stars rather than heated by shocks in supernova remnants (see, e.g., Telesco & Gezari 1992, and Ho et al. 1989 for the two alternative views, respectively). The grain size distribution is thought to be altered toward the smallward from the norm through mechanisms of destruction of the largest grains by grain-grain collisions in interstellar shocks driven by supernova remnants, although observational evidence for the occurrence of this process in Galactic supernova remnants is far from being ubiquitous (e.g., the review by Dwek & Arendt 1992). Some observational evidence consistent with a population of transiently heated small grains (probably depleted in the most intense areas of starbursts) comes out from the spatial variation of MIR color indices across the central regions of M82 (Telesco, Decher, & Joy 1989) and N253 (Piña et al. 1992), from the anomalously high 10 μm–to–thermal radio flux ratio (e.g., Wynn-Williams & Becklin 1985), and from the frequent presence of UIR emission bands in the nuclear MIR spectra of starburst nuclei (Roche et al. 1991). The UIR bands are generally attributed to emission by small grains or large molecules, like the polycyclic aromatic hydrocarbon (PAH) molecules (e.g., the review by Puget & Léger 1989); the UIR features are often absent in AGNs (Roche et al. 1991), probably because they are destroyed by the intense hard (EUV and X-rays) radiation field from the central source (Voit 1991, 1992).

4.8. *Relation between X-Rays and Mid-Infrared*

It is known that the 10 μm emission of galactic nuclei correlates with the radio continuum emission (e.g., Telesco 1988), with the near-infrared emission (e.g., Cutri & McAlary 1985; Devereux 1989; Lutz 1992), and with the far-infrared emission (at least for objects believed to be powered by starbursts; see, e.g., Scoville et al. 1983; Telesco 1988). In this subsection we wish to explore whether it also correlates with the X-ray emission in Seyfert galaxies, whose X-ray emission is generally dominated by a bright nuclear source. This issue has been very little discussed in the literature.

We have gathered together the soft X-ray fluxes F_{sX} of the Seyfert galaxies observed with the *Einstein Observatory* satellite (in common with our sample) from the compilation of Fabbiano, Kim, & Trinchieri (1992) (and references cited therein). Most of these X-ray data were obtained with the Image Proportional Counter instrument and in their catalog were converted into 0.2–4 keV fluxes. In the case of multiple entries for a galaxy we have adopted the mean values of the fluxes F_{sX}.

Owing to the presence of upper limits on the MIR data and to the smallness of the sample, we have used the Cox (C) and Kendall (K) correlation tests (mentioned in § 3) in order to compute the correlation probabilities between the fluxes F_N and F_{sX} for 14 Seyfert galaxies (N1068, N1365, N1386, N2992, N3227, N3783, N4051, N4151, N4388, N4639, N5506, N6814, N7213, N7582). We found no significant correlations. Figure 6 shows the log F_N–log F_{sX} plot. The study of the relation between the central MIR and the soft X-ray relation may be plagued by the fact that in some Seyfert galaxies the X-ray fluxes probably refer to a region larger than the area encompassed by the small-beam MIR observations. Observations with high spatial resolution in X-rays would be required to test adequately the MIR–X-ray correlation. Furthermore, internal obscuration of soft X-rays may be a potential source of considerable scatter in the correlation for both galaxy samples. But this is a minor problem, if it is true that X-ray–bright AGNs suffer, on average, less internal obscuration than X-ray–faint objects do (see, e.g., Reichert et al. 1985; Turner & Pounds 1989), perhaps because high-luminosity nuclei make a more hostile environment for absorbing matter.

Compared to soft X-rays, hard X-rays suffer little attenuation by interstellar matter and are good indicators of nonthermal emission because rapid variability and energy arguments imply that they originate very near the central engine. Turning to the X-rays of higher energies, we have considered basically the *HEAO 1* A-2 X-ray (2–10 keV) flux-limited sample of Piccinotti et al. (1982) (for N2992, N3783, N4151, N4593, N5506, N7172, N7213) complemented by the *HEAO 1* A-2 (2–10 keV) fluxes (F_{hX}) (or 2 σ upper limits) evaluated by Della Cecca et al. (1990) (for N1068, N3227, N3982, N4051, N5929). We have taken the average of the data for the first and second scan given by Piccinotti et al. (1982) in order to get fluxes in good agreement with those derived by Della Cecca et al. (1990) through a different procedure, except in the case of N3783 (for which we adopted the given upper limit). To this sample we have added the 2–10 keV fluxes of N4388 observed with the University of Birmingham X-ray telescope on the *Spacelab 2* mission (Hanson et al. 1990) and the

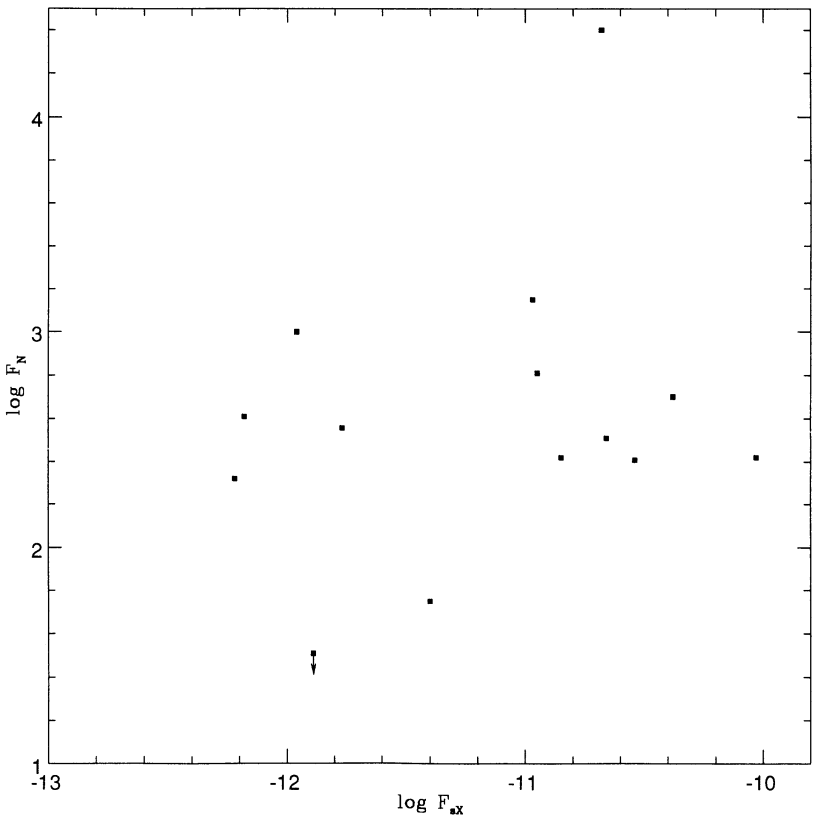

FIG. 6.—The log F_N–log F_{sX} plot, where the 10 μm fluxes F_N are in units of millijanskys and the soft X-ray fluxes F_{sX} are in ergs cm^{-2} s^{-1}. Upper limits are denoted by arrows.

average of the *HEAO 1* A-2 (2–20 keV) fluxes of the X-ray variable galaxy N6814 observed by Tennant et al. (1981) (The recent *Ginga* observations of N6814 yielded very similar 2–20 keV fluxes [Kunieda et al. 1990]). This sample of 15 Seyfert galaxies with hard X-ray data is hereafter referred to as sample A.

We have assembled another sample of hard X-ray data (hereafter referred to as sample B) substituting the data of Piccinotti et al. (1982) and Della Cecca et al. (1990) with the *EXOSAT* 2–10 keV fluxes (corrected for intrinsic and Galactic absorption) given by Turner & Pounds (1989). Although short- and long-term X-ray variability is a common phenomenon in AGNs, the fluxes do not generally vary by more than a factor of 2 (see, e.g., Grandi et al. 1992). Figures 7 and 8 illustrate the log F_N–log F_{hX} plot for samples A and B of 15 Seyfert galaxies. Owing to the presence of two cases of double censoring (both on F_N and F_{hX}) we have applied only the generalized Kendall tau test to the log F_N–log F_{hX}. Again we have detected no appreciable correlations between the fluxes. Table 4 contains the results of our correlation analysis (N_T is the total number of objects, N_L, N'_L, N''_L are the numbers of upper limits on the independent variable, dependent variable, and both variables, respectively).

TABLE 4

CORRELATIONS BETWEEN MIR AND X-RAY EMISSIONS

Correlation	Sample	N_T	N_L	N'_L	N''_L	p(C)	p(K)
log F_N–log F_{hX}.....	A	15	2	0	2	...	0.51
log F_N–log F_{hX}.....	B	15	0	0	2	...	0.16
log F_N–log F_{sX}.....	...	14	0	1	0	0.36	0.74

For AGNs, several authors have reported a correlation between the central near-infrared emission and the X-ray emission (see, e.g., the recent results of Kotilainen et al. 1992 and of Danese et al. 1992) and between the global far-infrared and X-ray emissions (e.g., Green, Anderson, & Ward 1992; David, Jones, & Forman 1992), although a close inspection of the paper by Green et al. (1992) reveals that the latter correlation is substantially induced by radio-loud quasars and disappears in a subsample of radio-quiet quasars and Seyfert galaxies. To our knowledge, there is only one paper (Carleton et al. 1987) in which the correlation between ground-based, small-beam 10 μm measures and X-ray emission is addressed. For a heterogeneous sample of detected AGNs (quasars and Seyfert galaxies), dominated by the X-ray–selected sample of Piccinotti et al. (1982), Carleton et al. (1987) claimed that the luminosities in the two bands correlate, in disagreement with our results (probably because his sample contains also several quasars).

The infrared–X-ray correlation is often cited as one of the main arguments supporting a nonthermal origin for most of the infrared continuum of AGNs (see, e.g., Bregman 1990 for relevant debates). The lack of correlation between the 10 μm and X-ray emissions of Seyfert galaxies is not in favor of the nonthermal origin of the MIR emission of Seyfert galaxies. (This conclusion may not hold for quasars.) Other arguments against the nonthermal model (specifically for the MIR emission of Seyfert galaxies) are the lack of MIR (as well as far-infrared) variability in radio-quiet quasars and Seyfert galaxies

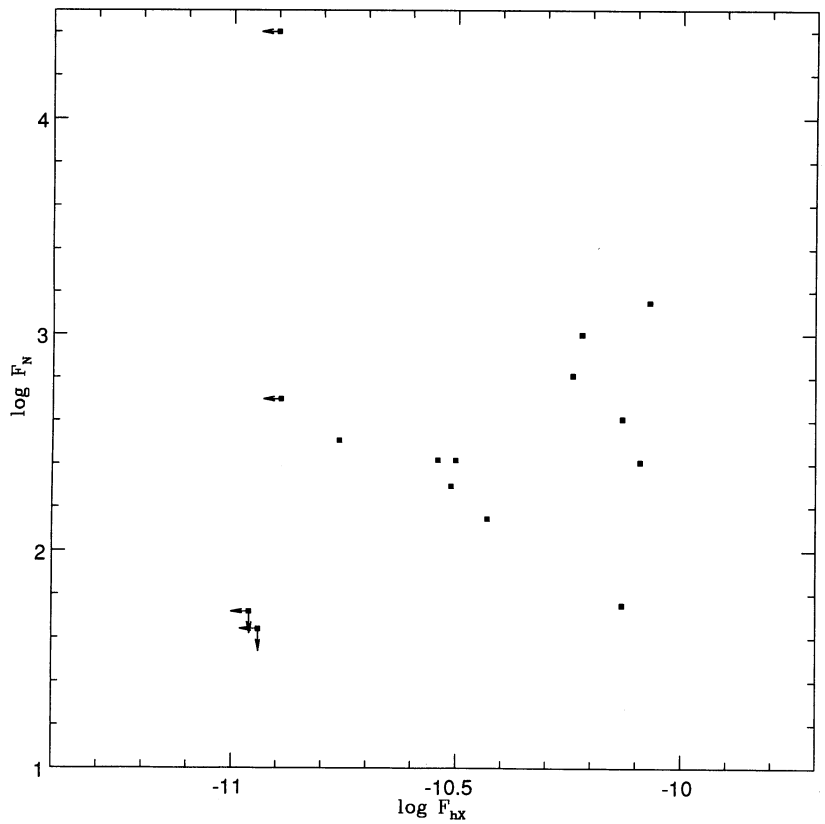

FIG. 7.—The log F_N–log F_{hX} plot, where the 10 μm fluxes F_N are in units of millijanskys and the hard X-ray fluxes are in ergs cm^{-2} s^{-1}, for sample A of Seyfert galaxies. Upper limits are denoted by arrows.

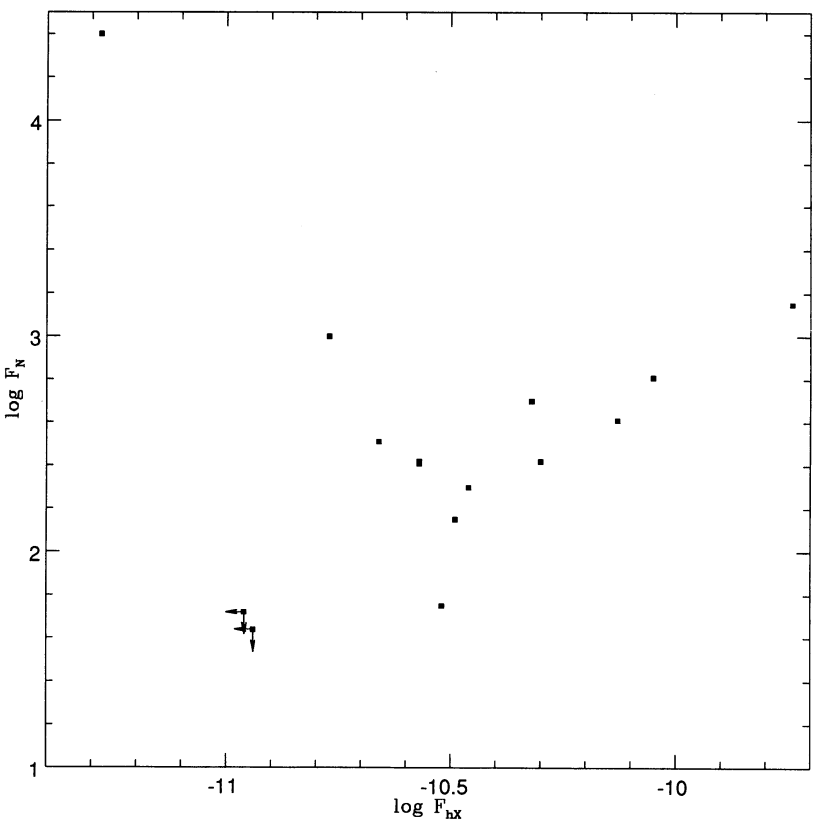

FIG. 8.—The log F_N–log F_{hX} plot, where the 10 μm fluxes F_N are in units of millijanskys and the hard X-ray fluxes are in ergs cm^{-2} s^{-1}, for sample B of Seyfert galaxies. Upper limits are denoted by arrows.

(Edelson & Malkan 1987; Neugebauer et al. 1989) and the sizes of the smallest nuclear MIR sources observed (see Telesco et al. 1984 for N1068 and Neugebauer et al. 1990 for N4151); these sizes are easily consistent with the order-of-magnitude predictions (~10–100 pc) of various models of thermal emission by central dust heated by the central continuum source (Barvainis 1987; Sanders et al. 1989; Laor & Draine 1993), whereas synchrotron models of MIR emission would require sources smaller than 10^{-4} pc.

5. CONCLUSIONS

Our statistical analysis has revealed a number of previously unrecognized features of the nuclear MIR emission of spiral galaxies. We summarize the main results of our study as follows:

1. The Seyfert galaxies contain the most powerful nuclear sources of 10 μm emission, which in approximately one-third of the cases provide the bulk of the emission of the entire galaxy; MIR emission in the outer regions is not uncommon in Seyfert galaxies.

2. Interacting nuclei are brighter at ~10 μm than noninteracting ones, although the effect is less pronounced than is generally believed. In addition, our study suggests that the enhancement in the central MIR emission may be essentially due to an increase of the central MIR surface brightness in the case of interacting LINERs and to a spread of the central MIR emission over a larger area in the case of interacting H II nuclei (similarly to the interaction-induced enhancement of the central radio emission of LINER and H II nuclei). The increased compactness of the 10 μm emission of interacting objects agrees with the similar behavior of several indices of star formation activity.

3. Among the non-Seyfert galaxies, H II region–like nuclei are, on average, stronger emitters at ~10 μm than normal nuclei (which confirms previous results) and than LINER nuclei, whose level of emission is not distinguishable from that of normal nuclei (this is a new result).

4. Early-type spirals have stronger and more compact 10 μm emission than late-type spirals.

5. Barred spirals have stronger and more compact 10 μm emission than unbarred systems, essentially because they more frequently contain H II nuclei.

6. Ringed and unringed spirals have similar central 10 μm emission.

7. The 10 μm emission of Seyfert galaxies appears to be unrelated to their X-ray emission, at variance with some previous claims.

The results of our detailed comparison between the behavior of various types of objects clearly emphasize that the 10 μm emission is particularly closely linked to the (predominantly nonthermal synchrotron) radio emission (at least at spatial scales of several hundreds parsecs).

The authors thank A. Biviano and M. Girardi for help in the statistical analysis and the referee J. C. Turner for constructive comments. The authors are grateful for the ASURV software package kindly provided by E. D. Feigelson. This work has been partially supported by the Italian Research Council (CNR-GNA) and by the Ministry of University, Scientific, and Technological Research (MURST).

REFERENCES

Avni, Y., Soltan, A., Tananbaum, H., & Zamorani, G. 1980, ApJ, 238, 800
Baldwin, J. A., Phillips, M. N., & Terlevich, R. 1981, PASP, 93, 5
Balzano, V. A. 1983, ApJ, 268, 602
Barvainis, R. 1987, ApJ, 320, 537
Becklin, E. E., et al. 1980, ApJ, 236, 441
Bothun, G. D., Lonsdale, C. J., & Rice, W. 1989, ApJ, 341, 129
Bregman, J. N. 1990, Astron. Ap. Rev., 2, 125
Buckley, J., & James, I. 1979, Biometrika, 66, 429
Bushouse, H. A. 1986, AJ, 91, 255
———. 1987, ApJ, 320, 49
Carico, D. P., et al. 1988, AJ, 95, 356
Carico, D. P., Sanders, D. B., Soifer, B. T., Matthews, K., & Neugebauer, G. 1990, AJ, 100, 70
Carico, D. P., et al. 1986, AJ, 92, 1254
Carleton, N. P., et al. 1987, ApJ, 318, 595
Cizdziel, P. J., Wynn-Williams, C. G., & Becklin, E. E. 1985, AJ, 90, 731
Condon, J. J., Condon, M. A., Gisler, G., & Puschell, J. J. 1982, ApJ, 252, 102
Cutri, R. M., & McAlary, W. 1985, ApJ, 296, 90
Dahari, O., & De Robertis, M. M. 1988, ApJS, 67, 249
Danese, L., et al. 1992, ApJ, 399, 38
David, L. P., Jones, C., & Forman, W. 1992, ApJ, 388, 82
Davis, L. E., & Seaquist, E. R. 1983, ApJS, 53, 269
Della Cecca, R., et al. 1990, ApJS, 72, 471
de Vaucouleurs, A., & Longo, G. 1988, Catalogue of Visual and Infrared Photometry of Galaxies, Monographs in Astronomy no. 5 (Austin: Univ. of Texas)
de Vaucouleurs, G., et al. 1991, Third Reference Catalogue of Bright Galaxies (New York: Springer) (RC3)
Devereux, N. A. 1987, ApJ, 323, 91
———. 1989, ApJ, 346, 126
Devereux, N. A., Becklin, E. E., & Scoville, N. 1987, ApJ, 312, 529
Durret, F. 1989, A&AS, 81, 253
Dwek, E., & Arendt, R. G. 1992, ARA&A, 30, 11
Edelson, R., & Malkan, M. 1987, ApJ, 323, 516
Edelson, R., Malkan, M. A., & Rieke, G. H. 1987, ApJ, 321, 233
Fabbiano, G., Kim, D.-W., & Trinchieri, G. 1992, ApJS, 80, 531
Feigelson, E. D., & Nelson, P. I. 1985, ApJ, 293, 192
Frogel, J. A., Elias, J. H., & Phillips, M. M. 1982, ApJ, 260, 70
Fullmer, L., & Lonsdale, C. J. 1989, Cataloged Galaxies and Quasars Observed in the *IRAS* Survey, 2d version (Pasadena: California Inst. Technology)
Giuricin, G., Bertotti, G., Mardirossian, F., & Mezzetti, M. 1990, MNRAS, 247, 444
———. 1991, MNRAS, 250, 392
Giuricin, G., Biviano, A., Girardi, M., Mardirossian, F., & Mezzetti, M. 1993, A&A, 275, 390
Giuricin, G., Mardirossian, F., & Mezzetti, M. 1988a, A&A, 194, 102
———. 1988b, A&A, 203, 39
Glass, I. S., & Moorwood, A. F. M. 1985, MNRAS, 214, 429
Glass, I. S., Moorwood, A. E. M., & Eichendorf, W. 1982, A&A, 107, 276
Graham, J. R., Wright, G. S., Meikle, W. P. S., Joseph, R. D., & Bode, M. E. 1984, Nature, 310, 213
Grandi, P., Tagliaferri, G., Giommi, P., Barr, P., & Palumbo, G. G. C. 1992, ApJS, 82, 93
Green, P. J., Anderson, S. F., & Ward, M. J. 1992, MNRAS, 254, 30
Hanson, C. G., Skinner, G. K., Eyles, C. J., & Willmore, A. P. 1990, MNRAS, 242, 262
Hawarden, T. G., Mountain, C. M., Leggett, S. K., & Puxley, P. J. 1986, MNRAS, 221, 41P
Heckman, T. M. 1990, in IAU Symp. 124, Paired and Interacting Galaxies, ed. J. W. Sulentic, W. C. Keel, & C. M. Telesco (NASA CP-3098), 359
Helou, G., Khan, I. R., Malek, L., & Boehmer, L. 1988, ApJS, 68, 151
Hill, G. J., Becklin, E. E., & Wynn-Williams, C. G. 1988, ApJ, 330, 737
Ho, P. T. P., Turner, J. L., Fazio, G. G., & Willner, S. P. 1989, ApJ, 344, 135
Hoel, P. G. 1971, Introduction to Mathematical Statistics (New York: Wiley)
Huchra, J., & Burg, R. 1992, ApJ, 393, 90
Hummel, E. E. 1981a, A&A, 93, 93
———. 1981b, A&A, 96, 111
Hummel, E. E., van der Hulst, J. M., Kennicutt, R. C., & Keel, W. C. 1990, A&A, 236, 333
Hunt, L. K. 1991, ApJ, 370, 511
Hurt, R. L., Merrill, K. M., Gatley, I., & Turner, J. C. 1993, AJ, 105, 121
Impey, C. D., Wynn-Williams, C. G., & Becklin, E. E. 1986, ApJ, 309, 572
Isobe, T., & Feigelson, E. D. 1990, BAAS (Software Reports), 22, 917
———. 1992, ApJS, 79, 197
Isobe, T., Feigelson, E. D., & Nelson, P. J. 1986, ApJ, 306, 490
Joseph, R. D., Meikle, W. P., Robertson, N. A., & Wright, G. S. 1984, MNRAS, 209, 111
Joseph, R. D., & Wright, G. S. 1985, MNRAS, 214, 87
Karachentsev, I. 1972, Comm. Spec. Astrophys. Obs., 7, 1
———. 1977, ApJS, 44, 137
Keel, W. C. 1983, ApJS, 52, 229

Keel, W. C. 1984, ApJ, 282, 75
Keel, W. C., Kennicutt, R. C., Hummel, E. E., & van der Hulst, J. M. 1985, AJ, 90, 708
Kotilainen, J. K., Ward, M. J., Boisson, C., DePoy, D. L., & Smith, M. G. 1992, MNRAS, 256, 149
Kriss, G. A., Canizares, C. R., & Ricker, G. R. 1980, ApJ, 242, 492
Kunieda, H., et al. 1990, Nature, 345, 786
Laor, A., & Draine, B. T. 1993, ApJ, 402, 441
Laurikainen, E., & Moles, M. 1989, ApJ, 345, 176
Lawrence, A., et al. 1985, ApJ, 291, 117
Lebofsky, M. J., & Rieke, G. H. 1979, ApJ, 229, 111
Lonsdale, C. J., Persson, S. E., & Mathews, K. 1984, ApJ, 287, 1009
Lutz, D. 1992, A&A, 259, 462
Mazzarella, J. M., & Balzano, V. A. 1986, ApJS, 62, 751
Moorwood, A. F. M., & Glass, I. S. 1984, A&A, 135, 281
Moorwood, A. F. M., Véron-Cetty, M.-P., & Glass, I. S. 1986, A&A, 160, 39
———. 1987, A&A, 184, 63
Neugebauer, G., Graham, J. R., Soifer, B. T., & Matthews, K. 1990, AJ, 99, 1456
Neugebauer, G., Soifer, B. T., Matthews, K., & Elias, J. H. 1989, AJ, 97, 957
Nilson, P. 1973, Uppsala General Catalogue of Galaxies (Uppsala Astron. Obs.)
Piccinotti, G., et al. 1982, ApJ, 253, 485
Piña, R. K., Jones, B., Puetter, R. C., & Stein, W. A. 1992, ApJ, 401, L75
Pogge, R. W. 1989, ApJ, 345, 730
Puget, J. L., & Léger, A. 1989, ARA&A, 27, 161
Reichert, G. A., Mushotzky, R. F., Petre, R., & Holt, S. S. 1985, ApJ, 296, 69
Rice, W., et al. 1988, ApJS, 68, 91
Rieke, G. H. 1976, ApJ, 206, L15
———. 1978, ApJ, 226, 550
Rieke, G. H., & Lebofsky, M. J. 1978, ApJ, 220, L37
———. 1979, ARA&A, 17, 477
Rieke, G. H., Lebofsky, M. J., Thompson, R. I., Low, F. J., & Tokunaga, A. T. 1980, ApJ, 238, 24
Rieke, G. H., & Low, F. J. 1972, ApJ, 176, L95
———. 1975, ApJ, 197, 17
Roche, P. F., Aitken, D. K., Phillips, M. M., & Whitmore, B. 1984, MNRAS, 207, 35
Roche, P. F., Aitken, D. K., Smith, C. H., & Ward, M. J. 1991, MNRAS, 248, 606
Rodriguez-Espinosa, J. M., Rudy, R. J., & Jones, B. 1987, ApJ, 312, 555
Sanders, D. B., Phinney, E. S., Neugebauer, G., Soifer, B. T., & Matthews, K. 1989, ApJ, 347, 29
Schmitt, J. H. R. M. 1985, ApJ, 293, 178
Schweizer, L. Y. 1987, ApJS, 64, 427
Scoville, N. Z., Becklin, E. E., Young, J. S., & Capps, R. W. 1983, ApJ, 271, 512
Soifer, B. T., Boehmer, L., Neugebauer, G., & Sanders, D. B. 1989, AJ, 98, 766
Spinoglio, L., & Malkan, M. A. 1989, ApJ, 342, 83
Stauffer, J. R. 1982, ApJS, 50, 517
Telesco, C. M. 1988, ARA&A, 26, 343
Telesco, C. M., Becklin, E. E., Wynn-Williams, C. G., & Harper, D. A. 1984, ApJ, 282, 427
Telesco, C. M., Decher, R., & Gatley, I. 1986, ApJ, 302, 632
Telesco, C. M., Decher, R., & Joy, M. 1989, ApJ, 343, L13
Telesco, C. M., & Gatley, I. 1981, ApJ, 247, L11
Telesco, C. M., & Gezari, D. Y. 1992, ApJ, 395, 461
Tennant, A. F., Mushotzky, R. F., Boldt, E. A., & Swank, J. H. 1981, ApJ, 251, 15
Tully, R. B. 1988, Nearby Galaxies Catalog (Cambridge: Cambridge Univ. Press)
Tully, R. B., & Shaya, E. J. 1984, ApJ, 281, 31
Turner, T. J., & Pounds, K. A. 1989, MNRAS, 240, 833
Ulvestad, J. S., Wilson, A. S., & Sramek, R. A. 1981, ApJ, 247, 419
van der Hulst, J. M., Krane, P. C., & Keel, W. C. 1981, AJ, 86, 1175
Véron-Cetty, M. P., & Véron, P. 1986, A&AS, 66, 335
———. 1991, A Catalogue of Quasars and Active Nuclei, 5th ed. (ESO Sci. Rep. 10)
Voit, G. M. 1991, ApJ, 379, 122
———. 1992, MNRAS, 258, 841
Vorontsov-Vel'yaminov, B. 1959, Atlas and Catalogue of Interacting Galaxies, Part 1 (Moscow: Moscow State Univ.)
———. 1977, A&AS, 28, 1
Ward, M., et al. 1987, ApJ, 315, 74
White, S. D. M., Huchra, J., Latham, P., & Davis, M. 1983, MNRAS, 203, 701
Willner, S. P., Elvis, M., Fabbiano, G., Lawrence, A., & Ward, M. J. 1985, ApJ, 299, 443
Wright, G. S., Joseph, R. D., Robertson, N. A., James, P. A., & Meikle, W. P. S. 1988, MNRAS, 233, 1
Wynn-Williams, C. G., & Becklin, E. E. 1985, ApJ, 290, 108
———. 1993, ApJ, 412, 535
Yamagata, T., Noguchi, M., & Iye, M. 1989, ApJ, 338, 707